



# CATÓLICA

## ESCOLA SUPERIOR DE BIOTECNOLOGIA

---

PORTO

### **DESIGN OF A DISPOSABLE $\mu$ PAD FOR ON-HAND QUANTIFICATION OF URINARY CREATININE**

by

Maria Manuel Pereira de Melo Rodrigues

September, 2022





# CATÓLICA

## ESCOLA SUPERIOR DE BIOTECNOLOGIA

---

PORTO

### **DESIGN OF A DISPOSABLE $\mu$ PAD FOR ON-HAND QUANTIFICATION OF URINARY CREATININE**

Thesis presented to Escola Superior de Biotecnologia of the Universidade Católica Portuguesa to fulfill the requirements of Master of Science degree in Biomedical Engineering.

---

by

Maria Manuel Pereira de Melo Rodrigues

**Supervisor:** Dr. Raquel B. R. Mesquita

**Cossupervisor:** Dr. António O. S. S. Rangel

September, 2022



## RESUMO

Neste projeto foi desenvolvido um novo dispositivo microfluídico baseado em papel ( $\mu$ PAD) para a quantificação de creatinina em amostras de urina. Quando comparado com outros métodos convencionais, este dispositivo inovador baseado em papel é mais acessível, portátil, e promove análises de baixo custo, podendo ser aplicado a fluídos biológicos não-invasivos. Para além disso, esta abordagem vai de encontro aos princípios de química-verde, uma vez que usa quantidades pequenas de reagentes, resulta numa produção de poucos resíduos, e pode ser descartado por inceneração.

A configuração deste dispositivo consistiu em duas camadas de papel de filtro com 9,5 mm de diâmetro, onde a camada superior serviu de reservatório e a camada inferior continha o reagente (solução alcalina de ácido pícrico). Esta unidade hidrofílica composta por uma dupla camada de discos, foi alinhada dentro de uma bolsa de plástico posteriormente laminada criando separação hidrofóbica, que continha furos de 3 mm para a inserção da amostra. Quando inserida, a creatinina presente nos padrões/amostras reage com o ácido pícrico (reação colorimétrica), e a cor dos discos muda de amarelo para cor-de-laranja/vermelho.

Após os estudos de otimização, o método desenvolvido permitiu uma quantificação de creatinina no intervalo dinâmico de 2.20-35.0 mg/dL, com um limite de deteção (LOD) de 0.66 mg/dL e um limite de quantificação (LOQ) de 2.20 mg/dL. A imagem é digitalizada ao fim de 20 minutos, sendo processada no software ImageJ, de modo a obter a intensidade de cor desenvolvida, que é depois convertida a pseudo-absorbância. A estabilidade do produto de reação, depois da inserção da amostra, foi verificada até 3 horas e o dispositivo pôde ser digitalizado dentro desse período de tempo. O  $\mu$ PAD permite obter curvas de calibração lineares até uma semana, quando armazenado em vácuo e colocado no frigorífico, a aproximadamente 4 °C.

Por fim, o método foi validado comparando os resultados obtidos com o dispositivo desenvolvido e um método de comparação, e foi demonstrado que não havia diferenças estatisticamente significativas entre eles. Assim sendo, foi possível concluir que este novo dispositivo foi desenvolvido com sucesso, uma vez que provou ser sensível e simples, assim como económico, visto custar cerca de 0.40 € (em termos de consumíveis).

**Palavras-chave:** Dispositivo microfluídico baseado em papel ( $\mu$ PAD); Determinação de creatinina; Amostras de urina; Reação Jaffe; Determinações em tempo real.



## ABSTRACT

In this work, a new microfluidic paper-based analytical device ( $\mu$ PAD) was developed for on-hand creatinine quantification in urine samples. When compared to other conventional methods, this innovative paper device is more accessible, portable, providing low-cost analysis and applicable to non-invasive biological fluids. Furthermore, this paper approach is environmentally friendly, as it uses small amounts of reagents, results in low waste production and it is disposable by incineration.

Its configuration consisted in two layers of filter paper discs of 9.5 mm of diameter, in which the top layer served as a reservoir and the bottom layer contained the reagent (alkaline picrate). This hydrophilic unit consisting of two-layer of filter paper was aligned within a laminated plastic pouch to set the hydrophobic separation, with 3 mm holes for the sample insertion. When inserted, creatinine of the standard/sample reacts with alkaline picric acid (colorimetric reaction), and the colour changes from yellow to orange/red.

Under optimal conditions, the developed method allowed creatinine quantification in the dynamic range of 2.20-35.0 mg/dL, with a limit of detection (LOD) of 0.66 mg/dL and a limit of quantification (LOQ) of 2.20 mg/dL. The image was scanned after 20 minutes and was processed in ImageJ software to obtain the colour intensity developed, later converted to pseudo-absorbance. The stability of the reaction product after the sample insertion was verified until 3 hours and the device could be scanned within that time. The  $\mu$ PAD allows to obtain linear calibration curves up to one week when stored in vacuum and placed in the fridge at approximately 4 °C.

Finally, the method was validated by the results obtained with the developed device and a comparison method, and it was demonstrated that there were no statistically significant differences between them. As so, it was possible to conclude that this novel device was successfully developed, as it proved to be sensitive and simple, as well as affordable, as it showed a cost of approximately 0.40 € (in terms of consumables).

**Keywords:** Microfluidic paper-based analytical device ( $\mu$ PAD); Creatinine determination; Urine samples; Jaffe reaction; Real time analysis.



## ACKNOWLEDGMENTS

First of all, I would like to thank my supervisor, Dr. Raquel Mesquita, for all the guidance and knowledge provided throughout the period of my thesis. For this, I am deeply thankful. Without her, I wouldn't be able to get this far and move forward to complete this work. Thank you for the patience with my micro-stress crises, for encouraging me, and for helping me see the bright side of things. To Dr. António Rangel, my cossupervisor, thank you as well for the trust in me and in this project. I am grateful for all the knowledge given in and out the laboratory, for the availability, and for assuring that I can do it. To both, I thank all the opportunities and the relentless support.

Also, I want to thank to my laboratory colleagues, Francisca, Juliana, Mafalda, Maria João and Tânia, for all the help and advice given during this journey and for turning the laboratory in an amazing and easy place to work in.

To all my close friends, thank you for giving me strength during this work, but also for helping me relax and making this time one of the happiest of my life. To my boyfriend, a special thank you for believing in me, for coping with my stress, for calming me down when I couldn't find a solution, and for always motivating me to do better.

Finally, I want to thank my family, especially my mother and father. You are my biggest supporters and none of this would be possible without the two of you. I am forever grateful for always encouraging me to follow my dreams and for always making me and my education a priority. I hope I made you proud and I will continue to do so.

In all these academic years, I went through a major evolution. I know I will be a great professional and I can guarantee that I am a better person. Therefore, I want to thank, lastly, to Escola Superior de Biotecnologia of Universidade Católica Portuguesa, for providing me this opportunity.



# CONTENTS

RESUMO.....	III
ABSTRACT.....	V
ACKNOWLEDGMENTS .....	VII
1. INTRODUCTION .....	1
1.1. Creatinine.....	1
1.1.1. Creatinine metabolism.....	1
1.1.2. Clinical significance of creatinine .....	3
1.1.3. Conventional creatinine testing and biological samples.....	3
1.1.4. Creatinine analysis - reaction with picric acid (Jaffe reaction).....	4
1.2. $\mu$ PADs - Microfluidic Paper-based Analytical Devices.....	6
1.2.1. Fabrication techniques.....	7
1.2.2. $\mu$ PAD detection methods and image analysis.....	9
1.3. Objectives.....	10
2. MATERIAL AND METHODS .....	11
2.1. Reagents and Solutions.....	11
2.2. Design and Assembly of the $\mu$ PAD .....	11
2.3. Creatinine Determination.....	12
3. RESULTS AND DISCUSSION .....	15
3.1. Preliminary Studies .....	15
3.2. $\mu$ PAD Physical Design .....	16
3.2.1. Top layer paper size .....	16
3.2.2. Top layer paper pore size.....	16
3.2.3. Top layer paper type .....	17
3.2.4. Bottom layer paper pore size.....	18
3.2.5. Bottom layer paper thickness .....	19
3.2.6. Order of layers.....	20
3.3. Colour Reaction Chemical Parameters Studies .....	21
3.3.1. Hydroxide concentration .....	21
3.3.2. Picric acid concentration .....	22
3.4. Standard/Sample Volume .....	23
3.5. Stability Studies and Features.....	25
3.5.1. $\mu$ PAD stability.....	25
3.5.2. Stability of the reaction product .....	26
3.5.3. Features of the $\mu$ PAD.....	27
3.6. Application to Samples.....	30

3.6.1.	Matrix interference assessment .....	30
3.6.2.	Accuracy assessment.....	31
4.	COST ANALYSIS .....	33
5.	CONCLUSION .....	34
6.	APPENDIX .....	36
7.	BIBLIOGRAPHY .....	40

## LIST OF FIGURES

Figure 1.1 - Molecules involved in creatinine formation. A - Creatine; B - Phosphocreatine; C – Creatinine, adapted from [6].	1
Figure 1.2 - Creatinine metabolism and its clearance rate in the kidney [16].	2
Figure 1.3 - Complex formed during the reaction between picric acid and creatinine (Jaffe reaction), adapted from [30].	4
Figure 1.4 - First introduced microfluidic paper-based device, for the detection of glucose and BSA protein, in 2007, adapted from [39].	6
Figure 1.5 - $\mu$ PAD fabrication using (A) Photolithography and (B) Method using only cut paper [41], [44].	9
Figure 1.6 - Colour intensity detection method example and corresponding analysis, adapted from [44].	10
Figure 2.1 - Schematic representation of the $\mu$ PAD assembly (A) Paper disc unit with two layers; (B) Insertion of the mixture reagent in the discs; (C) Paper disc alignment and laminating process, with the respective layers: L1, layer of the laminating pouch containing the holes for inserting the sample; E, empty layer; R, colour reagent solution layer; L2, bottom layer of the laminating pouch.	12
Figure 2.2 - Creatinine determination in the $\mu$ PAD. (A) Sample insertion and colour development after 20 minutes; (B) Scanning process, from the bottom (reagent) side; (C) ImageJ analysis of the scanned $\mu$ PAD, with the green (RGB) filter selected.	13
Figure 2.3 - Analysis of the intensities collected from the $\mu$ PAD and its absorbance calculation (example using one standard), along with the complete calibration curve obtained.	14
Figure 3.1 - Calibration curve obtained with the protocol used in a batch study (aqueous).	15
Figure 3.2 - Wheel of primary and complementary colours, used for the choice of the filter.	16
Figure 3.3 - Comparison of the sensitivity (calibration curve slope), for the top layer, using papers with different pore sizes; Error bars represent a 10% deviation.	17
Figure 3.4 - Comparison of the sensitivity (calibration curve slope), for the top layer, using papers of different types and 10 $\mu$ L of reagent; Error bars represent a 10% deviation.	18
Figure 3.5 - Comparison of the signal obtained, for the different bottom layer papers, in terms of their pore size; Green dots – Whatman 1; Blue dots – Whatman 4; Yellow dots – Whatman 5	19
Figure 3.6 - Comparison of the sensitivity (calibration curve slope), for the bottom layer, using papers with different thicknesses; Error bars represent a 10% deviation.	20
Figure 3.7 - Comparison of the sensitivity (calibration curve slope), for the different configurations of layers; Error bars represent a 10% deviation.	21

Figure 3.8 - Comparison of the sensitivity (calibration curve slope), for the different NaOH concentrations; Error bars represent a 10% deviation.....	22
Figure 3.9 - Comparison of the sensitivity (calibration curve slope) and correlation coefficient (black dots), for the different Picric Acid concentrations; Error bars represent a 10% deviation. ....	23
Figure 3.10 - Comparison of the sensitivity (calibration curve slope), for the different volumes of sample; Error bars represent a 10% deviation.....	24
Figure 3.11 - Comparison of the sensitivity (calibration curve slope), for the different volumes of sample; Error bars represent a 10% deviation.....	24
Figure 3.12 - Stability study of the $\mu$ PAD for the lower range of concentrations (0 to 15.0 mg/dL); Error bars represent a 10% deviation, and the black horizontal lines represent the range of the error bars with a 10% deviation.....	25
Figure 3.13 - Stability study of the $\mu$ PAD for the higher range of concentrations (15.0 to 35.0 mg/dL); Error bars represent a 10% deviation, and the black horizontal lines represent the range of the error bars with a 10% deviation.....	26
Figure 3.14 – Reaction product stability. Error bars represent a 5% deviation, and the black horizontal lines represent the range of the error bars with a 5% deviation. ....	27
Figure 3.15 - Comparison of the sensitivity (calibration curve slope) between H <sub>2</sub> O and Synthetic Urine, as well as the absorbance blank values for each matrix (black dots); Error bars represent a 10% deviation. ....	30

## LIST OF TABLES

Table 1.1 - Interfering compounds in the Jaffe reaction [32].....	5
Table 1.2 - Some $\mu$ PAD existing fabrication techniques, and their advantages and disadvantages [43].	8
Table 3.1 - Features of the developed $\mu$ PAD for creatinine determination in urine samples. ....	29
Table 3.2 – Comparison of the results obtained with the developed $\mu$ PAD and a comparative method (CM) by calculating the relative deviation percentage (%RD); SD, standard deviation.....	31
Table 4.1 - Price of the consumables used in the $\mu$ PAD and the total price per unit.....	33



# 1. INTRODUCTION

## 1.1. Creatinine

Creatinine is one of the natural compounds present in the body, which gives energy to the muscles and functions as an indicator of problems in the kidney, muscle, and thyroid [1]. It can be found in the serum but also in the secretions of the body, such as gastrointestinal fluids, bile, sweat [2] and urine.

This analyte is a waste product formed by the breakdown of creatine [3], and is produced predominantly in the muscle, but also in the pancreas, kidneys, and liver [3]. Furthermore, it has a phosphorylated form, phosphocreatine (Figure 1.1), which is responsible for the short-term storage of energy [4]. The levels of creatinine are usually constant in the human body and depend significantly on the muscle mass of each individual. Creatinine is mostly filtered by the kidney [5], and almost none of it is absorbed.

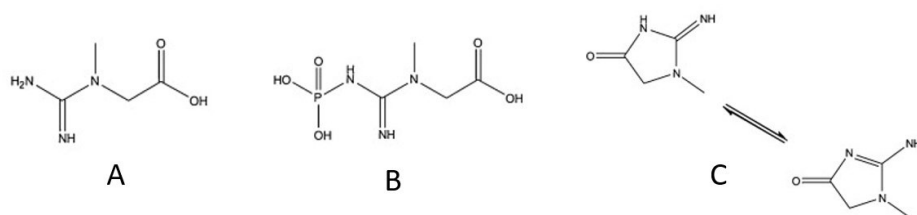


Figure 1.1 - Molecules involved in creatinine formation. A - Creatine; B - Phosphocreatine; C - Creatinine, adapted from [6].

### 1.1.1. Creatinine metabolism

In the human body, the normal levels of creatinine in blood vary [7] from 6 mg/L to 12 mg/L in adult men, and from 5 mg/L to 11 mg/L in adult women. Creatinine, as said, a waste product derived from muscle metabolism, is produced continuously, in resemblance of its secretion [8]. Therefore, in the kidney, creatinine is secreted almost completely, with “minimal tubular reabsorption”[9]. Due to this fact, kidney function can be assessed through the creatinine serum levels, but also through the amount of creatinine cleared, analysed by its range in urine. These values, when a sample of urine is collected randomly in a day, vary from 20 mg/dL to 320 mg/dL in men and, in women, from 20 mg/dL to approximately 280 mg/dL [10], while if the urine is tested in a full 24-hour test, the normal range is from 1.0 g to 2.0 g in men and 0.8 g to 1.8 g in women, during 24 h [11].

Assuming that the daily urine volume is 1,5 L [12], the range of creatinine in 24 h-urine tests, in mg/dL, is approximately 5-120 mg/dL. Even though the range of this analyte in urine samples is much wider than in serum samples, the first indicates better the changes that occurred in the kidneys' normal function [10].

The quantification of the analyte in a sample can indicate if the values are normal and correct, or if there is a health problem. However, to evaluate exactly the kidney function, the glomerular filtration rate (GFR) must be measured [13]. Since creatinine is filtered by the glomerulus, the GFR can be estimated by measuring the creatinine clearance, relating the serum creatinine levels with the urine volume and its concentration of creatinine [14], as it is represented in the following formula:

$$\text{Creatinine Clearance} = \frac{[\text{Creatinine}]_{\text{urine}} * \text{Volume}_{\text{urine}}}{[\text{Creatinine}]_{\text{serum}} * \text{Number of minutes of urine collection}}$$

Nevertheless, although creatinine clearance is a way to estimate approximately [15] the GFR, it has an inconvenience, which is the necessity of knowing the time of the urine collection and its accuracy [14]. Creatinine metabolism and its clearance rate in the kidney are represented in Figure 1.2.

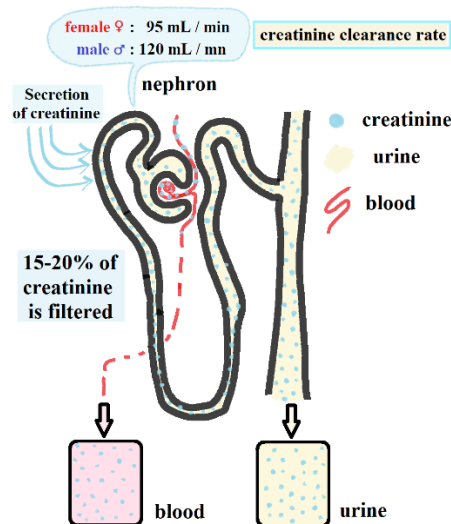


Figure 1.2 - Creatinine metabolism and its clearance rate in the kidney [16].

### **1.1.2. Clinical significance of creatinine**

As the levels of creatinine can indicate the existence of some problems, its monitorization is important to understand if the organism is working correctly. There are two cases of abnormality: if the creatinine is too low (lesser than the inferior limit), or if the creatinine is too high (higher than the superior limit).

On one hand, if the creatinine values in urine are too low, it can mean, mainly, that there are problems in the kidney and consequently, damage in the renal function. It is important to refer that creatinine decreasing in urine can also be related with nutritional factors, age, gender, and, therefore, subsequent muscle mass [17]. However, a chronic kidney disease [18] or a lower kidney function [19] can be related to these inferior values of the analyte in urinary excretions, independently of the factors named above. As so, if there is a kidney-associated disease, the glomerulus filtration capacity will be affected and there is no ability to concentrate urine at the maximum, which will reflect in less creatinine in the liquid excreted [20].

Furthermore, lower values can mean that the urine is more diluted than it is supposed to be, and the patient may be overhydrated [20]. Moreover, some drugs can influence and decrease the normal values of creatinine in urine, such as “antibiotic trimethoprim-sulfamethoxazole” and “H<sub>2</sub>-blocker cimetidine” that, by decreasing the secretion of creatinine, decrease its values in urine and subsequently, increase them in serum [21].

On the other hand, if the creatinine levels in urine are higher than expected, it may indicate dehydration [17] from the patient in question, because the urine is a lot more concentrated in creatinine and even other analytes. Additionally, the type of diet can increase urinary creatinine, specifically, when the diet is based on a higher intake of red meat and protein [17], [22], or when the individual consumes creatinine supplements. Another case where the creatinine values are superior to usual is when there is a hyperfiltration by the glomerulus. This happens when there is a pregnancy and also, if the renal plasma flow is normal but there is an increased filtration pressure (“glomerular hypertension”), it can represent the presence of type 2 diabetes mellitus [23].

### **1.1.3. Conventional creatinine testing and biological samples**

Creatinine values can be assessed through blood and urine samples, and these are the conventional means to obtain a sample to posterior quantification of the analyte.

For the blood test, a blood sample is collected from an arm vein, and, for the urine test, it is possible to do a 24h test, where the urine is collected throughout the day [24] and stored properly before analysis, or it can be a random test [25], where a urine sample is collected as usually is.

The urine samples are commonly collected and stored in a specific specimen collection cup, with an identifying label. Usually, 40 to 60 mL of urine are collected and, in terms of storage, the cup cap should be secure, and the sample has to be frozen at about  $-20^{\circ}\text{C}$  to guarantee its integrity [26].

#### 1.1.4. Creatinine analysis - reaction with picric acid (Jaffe reaction)

After having the urine samples, creatinine is determined, usually, through the Jaffe Reaction. The reaction was presented by Max Jaffe, about 130 years ago, and it is used until this day, due to the fact of being low cost, fast and simple. With this method, in an alkaline medium, a complex is formed (Figure 1.3), and the solution changes its colour from yellow to orange/red, which can be further analysed in a spectrophotometer and the present creatinine concentration is quantified [27][28]. This represents a colorimetric analysis, as the analyte in question is quantified through the colour change resulting from a certain reaction [29].

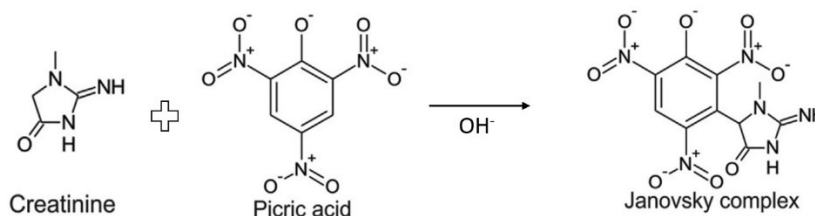


Figure 1.3 - Complex formed during the reaction between picric acid and creatinine (Jaffe reaction), adapted from [30].

This worldwide used method is affected by the concentration, temperature, wavelength of the measurement, and pH. Also, it has the disadvantage of interfering with some substances, such as glucose and aceto-acetate, which is possible to eliminate through an improvement of the method with an enzymatic reaction [31]. Specifying, the interfering compounds can influence the reaction itself, positively or negatively (influencing compounds), or can be artefacts related to urine or serum collection before the reaction between the creatinine present and picric acid (reactive compounds). Additionally, some substances can be considered as “apparent-creatinine”, as they don’t influence the reaction, but contribute to the colour formation [32]. Some of the compounds are identified in Table 1.1.

Table 1.1 - Interfering compounds in the Jaffe reaction [32].

<b>“Apparent-creatinine” compounds</b>	<b>Reactive Compounds</b>	<b>Influencing Compounds</b>	
		<b>Positive-Influence</b>	<b>Negative-Influence</b>
Acetone	Glucose*		
Acetoacetic acid*	Fructose	Adrenaline	Histidine
Adrenaline	Lactose	Ascorbic Acid	Glucose
Pyruvic acid	Urea	Glycylglycine anhydride	Guanidine compounds

\* The most interfering compounds are glucose and aceto-acetate, as the others are present in low concentrations (in blood).

However, the enzymatic improved method, despite being more specific, is ten times more expensive. The Jaffe conventional method still follows the analytical performance requirements and, therefore, this method will remain a relevant option in analysis, as well as the simplest of all methods developed so far [31], [33].

When preparing the solutions for this reaction, the pH should be alkaline, as mentioned, to allow the formation of that orange/red complex. Hence, to achieve the best colour for analysis in the spectrophotometer, in terms of intensity, the concentration of the chosen buffer solution, for example, sodium hydroxide, must be studied. First, this solution is added to picric acid to form alkaline picrate, which is then added to the creatinine solution for quantification [32].

In the spectrophotometer, the analyte quantification is through the measurement of the absorbance. Absorbance is the ability of a substance to absorb light, at a certain wavelength, [34] and there is a specific wavelength where the maximum absorbance is observed. For creatinine, the maximum absorbance appears at 490 nm but the linearity increases in the wavelength interval between 490 and 520 nm [28]. As the reaction is influenced by the concentration, with an increased creatinine concentration, the absorbance will also increase (more concentration, more absorbance). Regarding the picric acid concentration, the absorbance value will also increase, with a growth in the reagent concentration. However, when there is a change in picrate concentration above 0.005 M, even with a wide range of changing concentrations, it will not significantly influence the maximum value of absorbance [32].

## 1.2. $\mu$ PADs - Microfluidic Paper-based Analytical Devices

With the growth and development of new analysis systems, microfluidic devices have taken an important place because this type of equipment uses small volumes in small dimensions, miniaturized equipment, and it is fast and non-expensive [35], which fits the guidelines of World Health Organization, in the “ASSURED”. In other words, these devices are “affordable, sensitive, specific, user-friendly, rapid, robust, equipment-free and deliver-able to end users” [36], allowing to move forward in analytical chemistry, biology, and medicine [35].

The first paper-based microfluidic device was invented in 2007 by Whitesides [37][38], with the ability to detect glucose and protein in urine, in a disposable, small, and easy-to-use way. It used a chromatography paper patterned with a photoresist material and, with the proper reagents, the detection of both compounds was successful (Figure 1.4), concluding also that this assay could be used for other analytes [39].

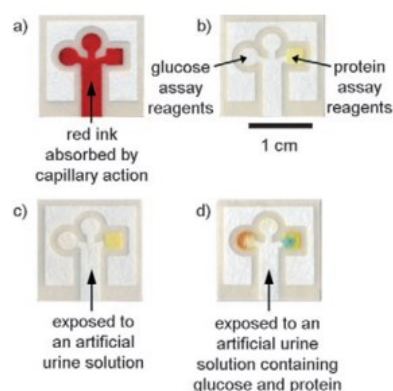


Figure 1.4 - First introduced microfluidic paper-based device, for the detection of glucose and BSA protein, in 2007, adapted from [39].

In the following years, this field has continuously grown and  $\mu$ PADs are now used in various areas. In general, conventional microfluidic devices and novel  $\mu$ PADs have hydrophilic areas, provided by the paper zones, and hydrophobic areas surrounding them [40]. On one hand, conventional devices use materials like glass, silicon, and polymers [37], [38], and techniques to pattern paper like wax printing and photolithography [40]. On the other hand, although new  $\mu$ PADs seem to not have the mechanical robustness present in conventional microfluidic devices, the use of only paper, observed in this kind of biosensors, is a huge advantage, since it makes this method much cheaper and more available to the end-user, as well as lightweight, simple, and easy for transportation and storage [37], [41].

Furthermore, the paper can be of different types, including graphite, chromatography, and filter paper, all composed of cellulose, that has a good capillary and immobilization action of different substances [38], compatible with biological samples. Also, the paper can have various options of porosity and thickness [41], [42], which makes the  $\mu$ PADs an innovative way of analysis, adaptable to different important analytes.

### **1.2.1. Fabrication techniques**

There are 2D and 3D fabrication methods, depending on the analysis, in terms of their complexity [38]. The 2D devices are characterized for having horizontal flow in multiple directions and the 3D ones can have a vertical flow [43]. When folding or bending the 2D-configuration, by stacking, for example, layers of paper, a 3D-configuration is achieved [40], [43].

In each configuration, the well-defined hydrophobic and hydrophilic areas can be obtained by patterning the paper, to obtain the hydrophobic barrier, or shape and cutting the paper, to define the hydrophilic barrier relatively to the hydrophobic zone [41], [43]. Some of the techniques used in the fabrication of these  $\mu$ PADs are presented in Table 1.2, along with their advantages and disadvantages.

Table 1.2 - Some  $\mu$ PAD existing fabrication techniques, and their advantages and disadvantages [43].

<i>Fabrication technique</i>	<i>Advantages</i>	<i>Disadvantages</i>
<b>Photolithography</b>	Patterned paper with photoresist materials with high resolution and simple fabrication.	Quite expensive due to the fact of equipment and reagent requirements, as well as complex procedures.
<b>Inkjet printing</b>	Patterned paper with AKD (alkenyl ketene dimer), methylsilsequioxane, UV curable acrylates with customizable ink material, and high throughput.	The printer used must be modified and the life of the equipment can be compromised, which may become more expensive.
<b>Wax printing</b>	Patterned paper with wax, while having a simple fabrication and high throughput.	Expensive wax, that requires being printed, and influences the method and its resolution.
<b>Cutting</b>	Does not require a patterning agent and has high resolution and throughput.	Requires a cutter (crafted or laser) and has low mechanical stability.
<b>Laser etching</b>	Does not require a patterning agent and has high resolution and throughput.	Requires a CO <sub>2</sub> laser cutter and the paper must be omniphobic or have a silanization treatment.

A representation of the  $\mu$ PAD fabrication using photolithography method in paper patterning (to create the hydrophobic barrier), as well as a method using only cut paper (delimited by a hydrophobic material), is observed in Figure 1.5.

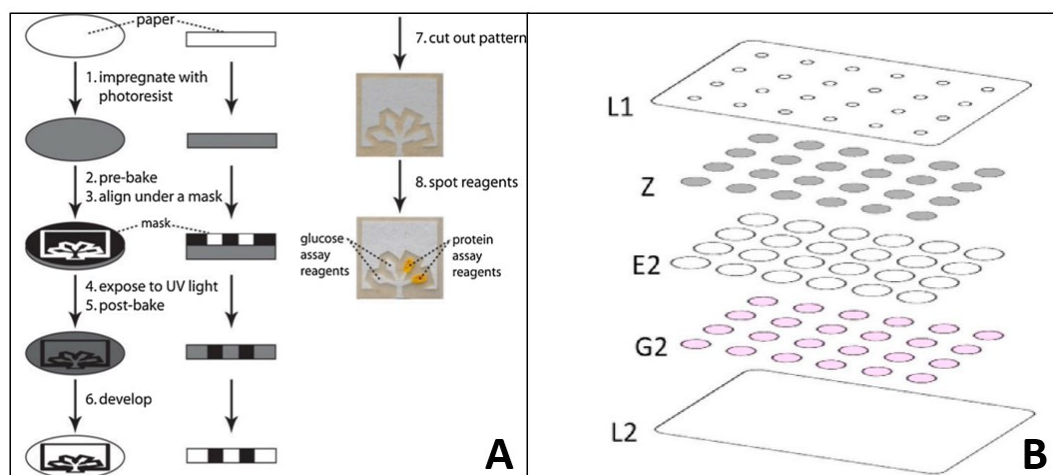


Figure 1.5 -  $\mu$ PAD fabrication using (A) Photolithography and (B) Method using only cut paper [41], [44].

### 1.2.2. $\mu$ PAD detection methods and image analysis

In addition to the inexpensive assembly of the  $\mu$ PADs, its analysis is also cheap, since these devices are usually used with colorimetric analysis [44]. This type of reaction, due to the development of colour change, presents different intensities that can be analysed with low-cost scanners, digital cameras, or mobile phones, and with further image analysis software [45].

The colorimetric tests in  $\mu$ PADs can be qualitative, semi-quantitative, and quantitative. Qualitative is when the device can give a result only by the colour change, associated with yes or no results and naked eye analysis. A semi-quantitative test can be the use of a colour chart, given by a calibration curve, to estimate the quantity of the analyte. But, when using an image-analysis and processing software, after the  $\mu$ PAD scanning, it is a question of a quantitative assay, where a precise quantity of the analyte is determined [37], [42].

This type of equipment can reach the analytical requirements of a conventional UV-VIS spectrophotometry method, but it has the advantage of being portable and cheaper while using a significantly smaller volume of sample. A calibration curve is easily obtained by inserting standard solutions into the  $\mu$ PAD, which will lead to a colour development related to each standard concentration, determined by this colorimetric analysis [45]. After obtaining the image of the  $\mu$ PAD, after scanning or capturing a picture, a program like Adobe Illustrator, ImageJ or Photoshop® is used to analyse the colour intensity. [40], [44].

For this purpose, an RGB system is used to collect the intensity of the coloured zones [42], and one filter channel corresponding to the colours Red, Green and Blue is chosen, by being the closest complementary colour of the colour developed after the reaction [40], [46].

This will allow for the intensity values to be converted into a sort of absorbance value. The average colour intensity in each detection area is determined, with the image processing software and RGB filters, and the values used for each absorbance calculation are the intensities of the blank solution, as well as the intensities of the standard/sample solutions in question [47], [48]. This reflects on the Beer-Lambert law, and the absorbance is calculated using the formula:

$$A = \log_{10} \left( \frac{I_0}{I} \right)$$

Where the A is absorbance value,  $I_0$  is the colour intensity obtained by the average intensity of the blank solutions and I is the average colour intensity obtained by the standard or sample solutions [40]. After having this information, the data is transferred to Microsoft Excel to obtain the corresponding calibration curve [45].

This kind of analysis (absorbance spectroscopy), has been proven to provide sensitive results in the quantification of analytes in microfluidic paper-based devices, and an example of this data collection method can be observed in Figure 1.6 [37].

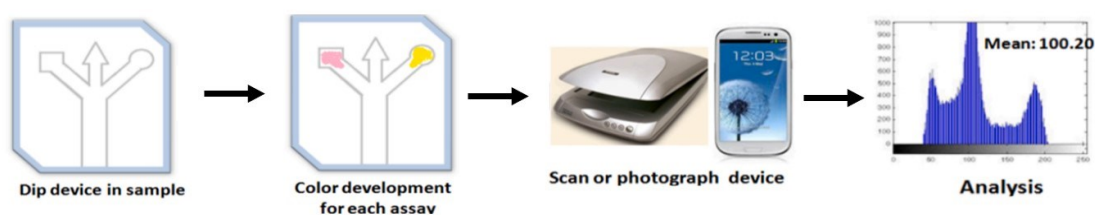


Figure 1.6 - Colour intensity detection method example and corresponding analysis, adapted from [44].

### 1.3. Objectives

With the growth of the medical and biomedical field, there is an urgency to find new, fast, and simple methods to determine important chemical compounds, that are present in the human body. As so, the objective was to devise a method for the inexpensive, portable, disposable and in the moment determination of creatinine, for the diagnosis of kidney-associated issues, with the fabrication of a microfluidic paper-based analytical device ( $\mu$ PAD).

## 2. MATERIAL AND METHODS

### 2.1. Reagents and Solutions

The solutions were all prepared with analytical grade chemicals and Milli-Q® Water (Resistivity > 18 MΩ•cm, Millipore, Bedford, MA, USA).

The picric acid solution was prepared weekly, by dissolving 57 mg of picric acid (Sigma) in 5.00 mL of water (0.050 M).

A sodium hydroxide stock solution was obtained by dissolving 10 g of sodium hydroxide (PanReac) in 50.0 mL of water, resulting in a 5.0 M solution. Then, the hydroxide buffer solution was prepared, by dilution of the stock solution to a concentration of 2.0 M.

The colour reagent solution was prepared daily to be used in the Jaffe reaction with creatinine: 240 µL of picric acid 0.050 M were mixed with 60.0 µL of NaOH 2.0 M, resulting in a 0.040 M of picric acid and 0.40 M of NaOH [49], [50] in the working reagent solution.

A creatinine stock solution of 1000 mg/L was prepared every other day, by dissolving 10.0 mg of creatinine (Sigma) in 10.0 mL of water. Afterwards, from this solution, the working standards were obtained, within a range of 25.0 mg/L to 350 mg/L (2.50 mg/dL to 35.0 mg/dL).

### 2.2. Design and Assembly of the µPAD

The µPAD design consists in two hydrophilic layers of different types of filter paper, to create vertical flow. The two-layer unit (hydrophilic area) is separated from the hydrophobic zones with the use of plastic laminating pouches (75 x 110 x 0.125 mm, Q-Connect, Gent, Belgium). Each plastic pouch has one side with 24 holes cut out, containing 6 columns and 4 rows of the two-layer discs.

For the two-layer unit (Figure 2.1, (A)), filter paper discs are cut with 9.5 mm diameter (3/8" EK tools, Lindon, USA). The top layer, without the addition of any solution (reservoir), consists in a qualitative filter paper (Whatman® W1), while the bottom layer contains the reagent and consists in a hardened ashless filter paper (Whatman® W542).

First, the reagent layer (bottom layer) was prepared by loading 12 µL of colour reagent in the W542 filter paper disc, as shown in Figure 2.1 (B). Then, the discs were placed in the oven to dry (at 50°C for 10 minutes),

Afterwards, the two-disc layers were aligned into the plastic pouch, followed by a sealing process through lamination (ACCO Brands Europe, Style/CBT12698), to create the proper hydrophobic and hydrophilic zones (Figure 2.1 (C)).

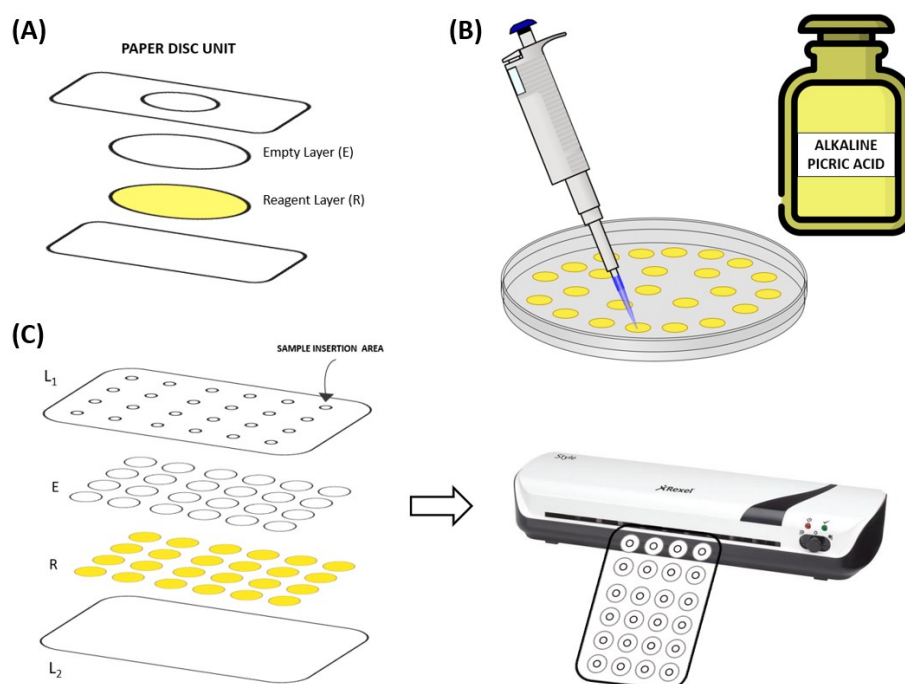


Figure 2.1 - Schematic representation of the  $\mu$ PAD assembly  
 (A) Paper disc unit with two layers; (B) Insertion of the mixture reagent in the discs; (C) Paper disc alignment and laminating process, with the respective layers: L<sub>1</sub>, layer of the laminating pouch containing the holes for inserting the sample; E, empty layer; R, colour reagent solution layer; L<sub>2</sub>, bottom layer of the laminating pouch.

### 2.3. Creatinine Determination

To determine the creatinine concentration, it was inserted 15  $\mu$ L of the standard (or sample) solution into the top layer disc, through a previously made hole in the plastic pouch, of 3 mm (Figure 2.2 (A)). Then, after 20 minutes of waiting, to promote the colour development, the sample holes were covered with tape and the  $\mu$ PAD was scanned (Canon LIDE 120), on the side of the reagent layer, in order to analyse the intensity of each disc (Figure 2.2 (B)). To measure this colour intensity, the software used was ImageJ. In this software, the intensity value can be obtained using RGB filter (red, green, and blue filters), and, for this case in specific, the green filter was use as complementary colour of the formed product (Figure 2.2 (C)).

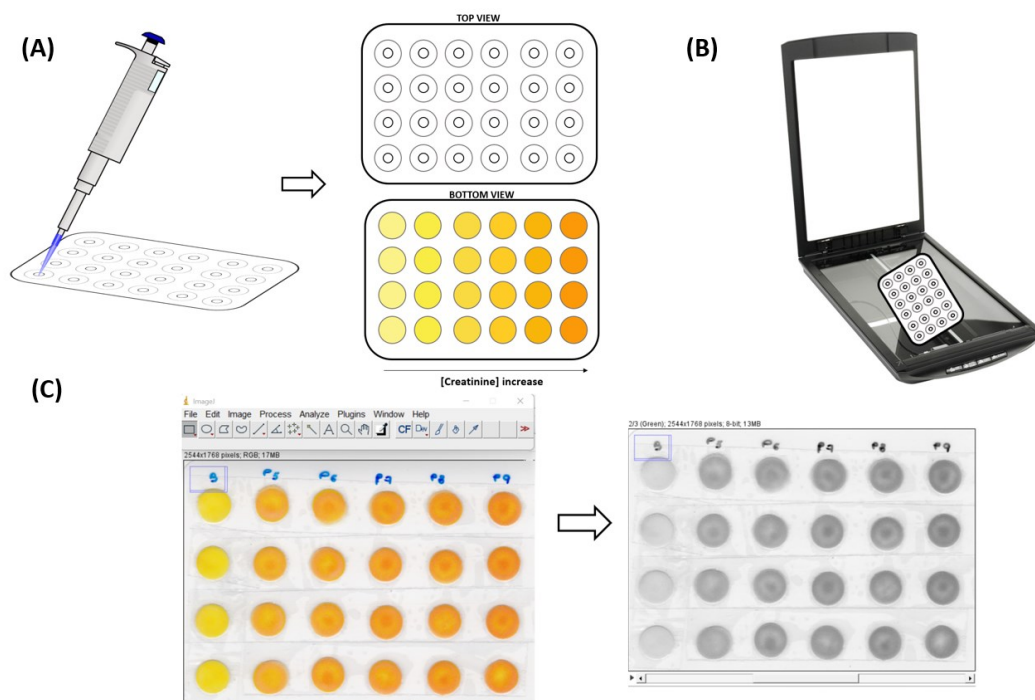


Figure 2.2 - Creatinine determination in the  $\mu$ PAD.  
 (A) Sample insertion and colour development after 20 minutes; (B) Scanning process, from the bottom (reagent) side;  
 (C) ImageJ analysis of the scanned  $\mu$ PAD, with the green (RGB) filter selected.

After having the intensity values of all discs in the  $\mu$ PAD, the data was imported to Microsoft Excel (version 2206), for posterior analysis. All intensity values, organized in standards/samples, were converted to absorbance. Therefore, the absorbance of each solution was calculated as explained before (Section 1.2.2). Then, a calibration curve was subsequently obtained, by relating each standard concentration to each value of absorbance calculated, as represented in Figure 2.3. Consequently, this allowed, by also analysing the colour intensity of a specific sample, to determine the analyte concentration in it, using the equation obtained in the calibration curve.

	∅	Area	Disc Mean Intensity	Absorbance
Branco	1	39765	213.085	-0.0040
	2	39765	209.283	0.0040
	3	39765	209.713	0.0030
	4	39765	212.519	-0.0030
P5	5	39765	173.747	0.0850
	6	39765	172.897	0.0870
	7	39765	171.887	0.0800
	8	39765	176.78	0.0770

ABSORBANCE CALCULATED USING BEER-LAMBERT LAW



[Creatinine], mg/dL	Average Absorbance
0.00	0.000
15.00	0.0830



COMPLETE CALIBRATION CURVE  
mg/dL

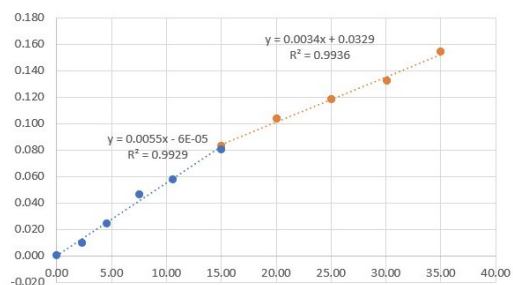


Figure 2.3 - Analysis of the intensities collected from the  $\mu$ PAD and its absorbance calculation (example using one standard), along with the complete calibration curve obtained.

To validate the developed method, the results collected from the sample analysis in the  $\mu$ PAD were compared with a batchwise procedure done in urine samples, according to Sitanurak et al [50].

### 3. RESULTS AND DISCUSSION

#### 3.1. Preliminary Studies

To develop this device, it was necessary to study the best combination of the solutions involved in the Max Jaffe reaction, given the fact that this was the reaction chosen for the creatinine determination. The protocol chosen initially used picric acid with 0.03 M, previously mixed with NaOH of 0.4 M [49]. This was first evaluated by a batch study with aqueous solutions, where the calibration curve presented an increased absorbance with an increased concentration of creatinine, after waiting 20 minutes, with good sensitivity and linearity, as shown in Figure 3.1.

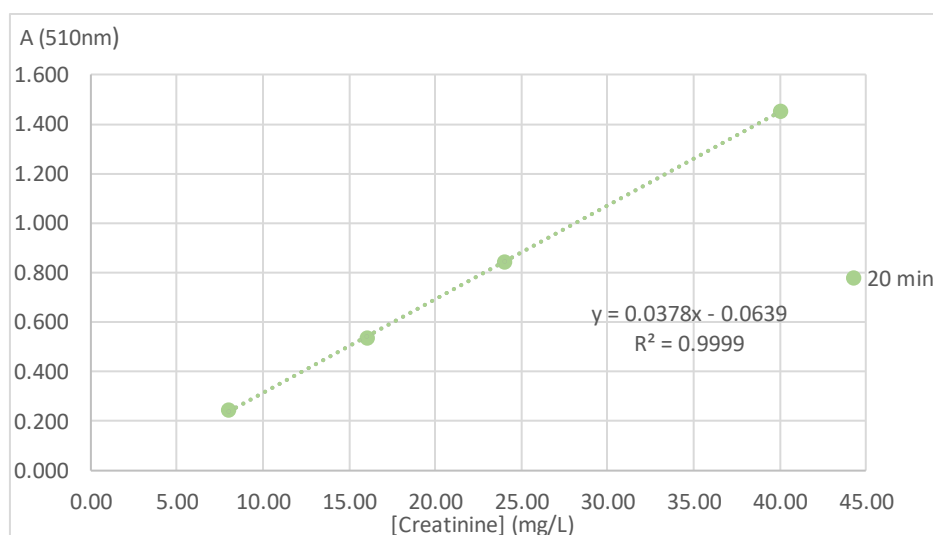


Figure 3.1 - Calibration curve obtained with the protocol used in a batch study (aqueous).

In this batchwise study, other waiting times were studied but 20 minutes resulted in higher sensitivity than intervals of time (such as 5 and 10 minutes), and 30 minutes didn't show significant changes in sensitivity.

When transferring the reaction to paper, the physical design of the  $\mu$ PAD, namely the number of layers, and chemical parameters, namely the amount of reagent, were studied. Furthermore, the determination of creatinine is calculated by interpolation in calibration curves, established between the creatinine concentration of standards and the calculated absorbance, which was only possible after scanning and image processing with ImageJ. The RGB filters green and blue, used to measure the colour intensity developed in the device, were compared.

Blue and green are the basic colours closer to the (complementary) colours present in the  $\mu$ PAD (yellow turned into orange-red), as shown in Figure 3.2.

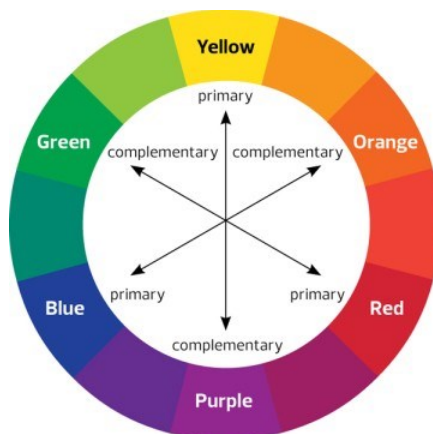


Figure 3.2 - Wheel of primary and complementary colours, used for the choice of the filter.

The filter chosen was the green filter, as mentioned, due to the fact of having more sensitivity and the standards showed more differences in intensities between each other.

### 3.2. $\mu$ PAD Physical Design

Initially, the  $\mu$ PAD was assembled using 2 layers of Whatman 1, one on the top with 15  $\mu$ L of colour reagent (following protocol proportions), and the other an empty disc used as a reservoir (bottom). The device was scanned from the top part and the intensity was read in the top disc, after inserting 20  $\mu$ L of sample and a reaction time of 20 minutes.

#### 3.2.1. Top layer paper size

Two-disc sizes were compared for the top layer, one of 9.5 mm, and one of 12.7 mm, using a 12.7 mm disc for the bottom layer. When scanning the  $\mu$ PAD after the reaction, the one with 9.5 mm in the top layer resulted in a sensitivity increase (calibration curve slope 82% higher). This might occur as a smaller-sized disc can concentrate more the reagent before the reaction.

#### 3.2.2. Top layer paper pore size

Having a top layer with 9,5 mm of dimension, the pore size of the layer was also studied. The paper Whatman 1 (pore size 11  $\mu$ m), the paper Whatman 4 (pore size 20 to 25  $\mu$ m), and the paper Whatman 5 (pore size 2.5  $\mu$ m) were compared.

After analysing these results (Figure 3.3), the Whatman 5 was chosen as it presented more sensitivity since a smaller pore indicates fewer particles go through the layer, which results in more time for the reaction to occur in this top layer.

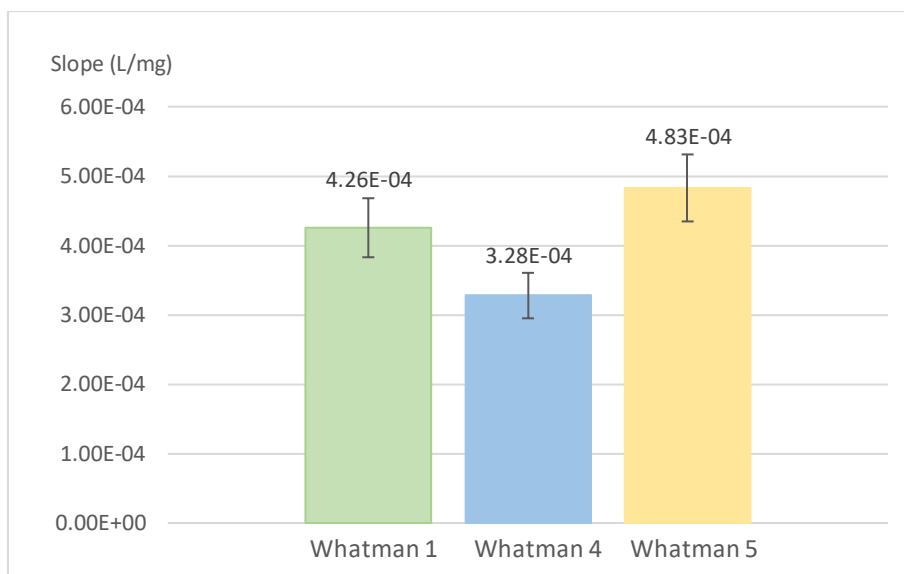


Figure 3.3 - Comparison of the sensitivity (calibration curve slope), for the top layer, using papers with different pore sizes; Error bars represent a 10% deviation.

### 3.2.3. Top layer paper type

To improve the device, besides studying the size and the pore of the reagent layer, the type of paper (treatment) was also studied to verify which paper property is more suitable for this reaction. Maintaining the pore of approximately  $2.5 \mu\text{m}$ , a qualitative paper (Whatman 5) was compared with an ashless quantitative paper (Whatman 42), a hardened low ash paper (Whatman 50), and a hardened ashless paper (Whatman 542).

The first comparison test was done with the addition of  $15 \mu\text{L}$  of reagent and the  $\mu\text{PAD}$  with the papers Whatman 50 and Whatman 542 presented more sensitivity. However, this study can't be validated because this volume overflowed in these papers with different treatments. As so, a reagent volume of  $10 \mu\text{L}$  was tested and, in this case, the more sensitive was, significantly, the Whatman 542, as shown in Figure 3.4.

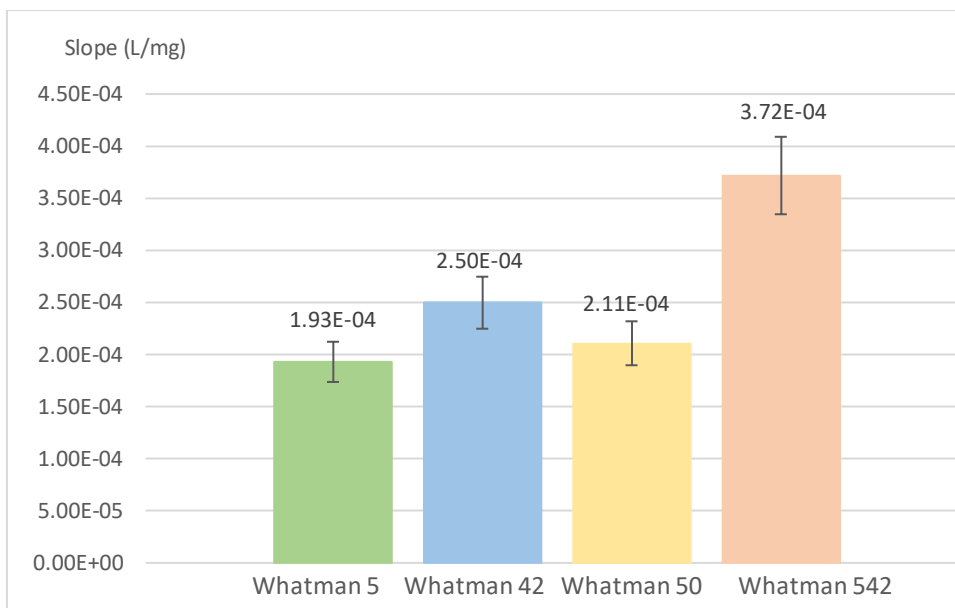


Figure 3.4 - Comparison of the sensitivity (calibration curve slope), for the top layer, using papers of different types and 10  $\mu\text{L}$  of reagent; Error bars represent a 10% deviation.

To further enhance the device performance, a reagent volume of 12  $\mu\text{L}$  was then tested with the Whatman 542, to have more reagent and, subsequently, higher sensitivity (calibration curve slope). In the end the paper chosen was the Whatman 542 with 12  $\mu\text{L}$ .

### 3.2.4. Bottom layer paper pore size

After studying and improving the top layer, the bottom layer was also studied. The first parameter studied was also the pore size. Using a top layer with Whatman 542, the paper Whatman 1, 4, and 5 were compared for the bottom layer, and the calibration curves obtained are presented in Figure 3.5.

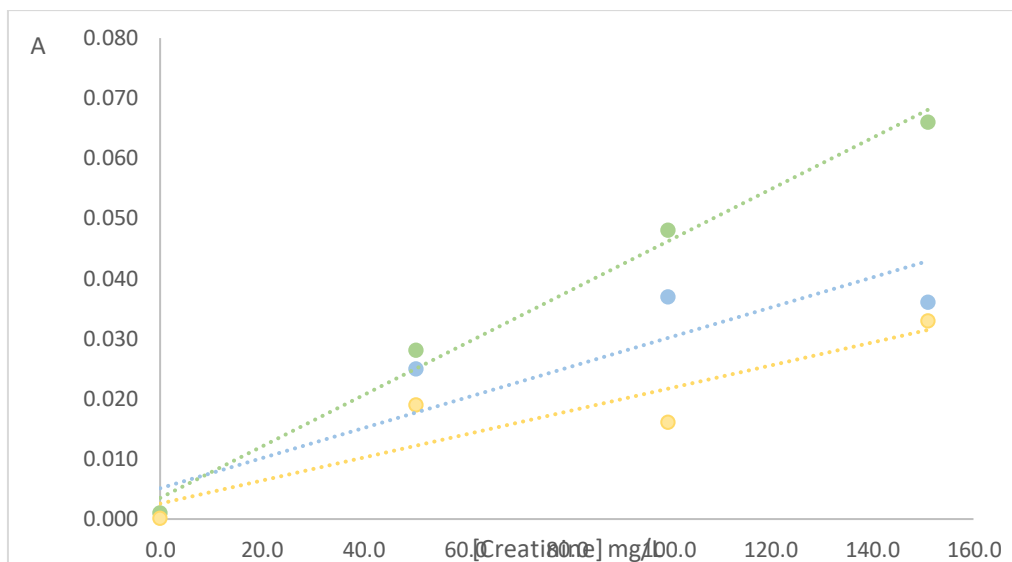


Figure 3.5 - Comparison of the signal obtained, for the different bottom layer papers, in terms of their pore size; Green dots – Whatman 1; Blue dots – Whatman 4; Yellow dots – Whatman 5

Given the fact that the calibration curve marked with green dots was the only one that presented linearity, the paper chosen was Whatman 1.

### 3.2.5. Bottom layer paper thickness

Another physical parameter studied was the thickness of the filter paper in the bottom layer. The intention of carrying out this study was to enable testing higher sample volume. To increase the sample volume, the thickness also needed to be increased, to absorb a higher volume of sample that, expectably, reflects in an improvement of the  $\mu$ PAD sensitivity (Figure 3.6).

So, filter papers Whatman 1 (W1\_20 $\mu$ L\_20min) and Whatman 3 (W3\_20  $\mu$ L\_20min) were compared, since they are both qualitative papers and presented approximately the same pore size but different thicknesses, 0.18 and 0.39 mm, respectively. Additionally, while using Whatman 3, since it was thicker, the sample volume was increased to 25  $\mu$ L (W3\_25 $\mu$  \_20min) and for the same volume of 20  $\mu$ L the reaction time was decreased in half (W3\_20 $\mu$ L\_10min).

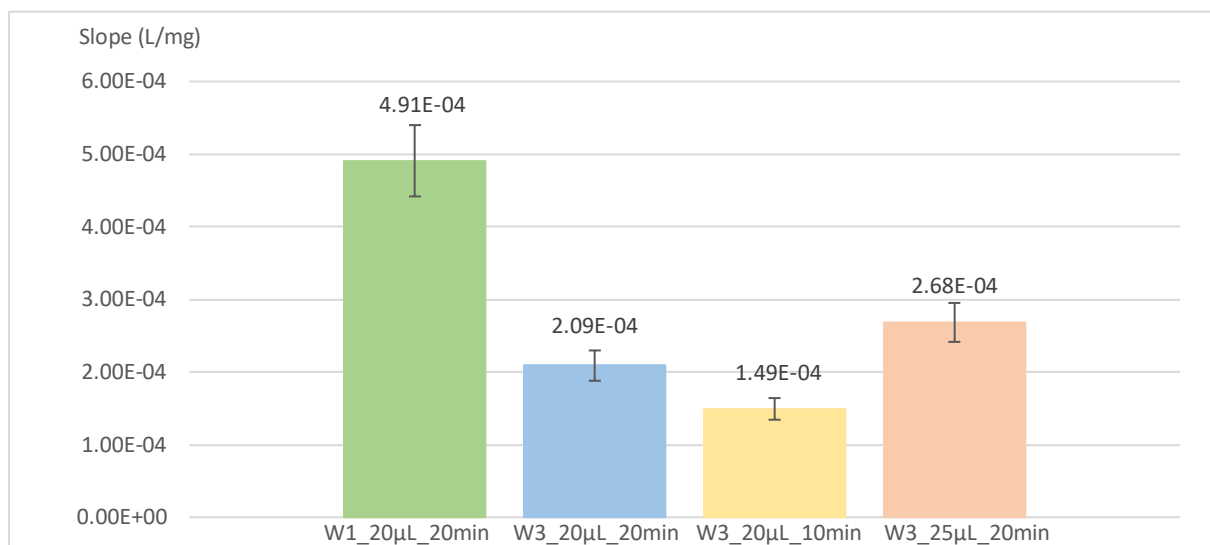


Figure 3.6 - Comparison of the sensitivity (calibration curve slope), for the bottom layer, using papers with different thicknesses; Error bars represent a 10% deviation.

The higher sensitivity was obtained when using Whatman 1 in the bottom layer, even comparing to more sample volume (with an increased thickness) so this filter paper type was chosen.

### 3.2.6. Order of layers

After deciding the type of filter paper used for each layer, the order of layers was also studied. This study was performed mainly because the reagent was initially in the top layer and transferring it to the bottom layer could be more advantageous, as it would be more protected. Thus, the initial configuration (Top Layer: colour reagent (9.5 mm, W542), 20 µL of sample; Bottom Layer: reservoir (12.7 mm, W1), 20 minutes) was compared with other configurations using the same paper types. When testing the empty layer on top (inverted configuration) a smaller size of the paper disc was also tested (inverted configuration\_small) which implied a smaller volume (15 µL) (Figure 3.7).

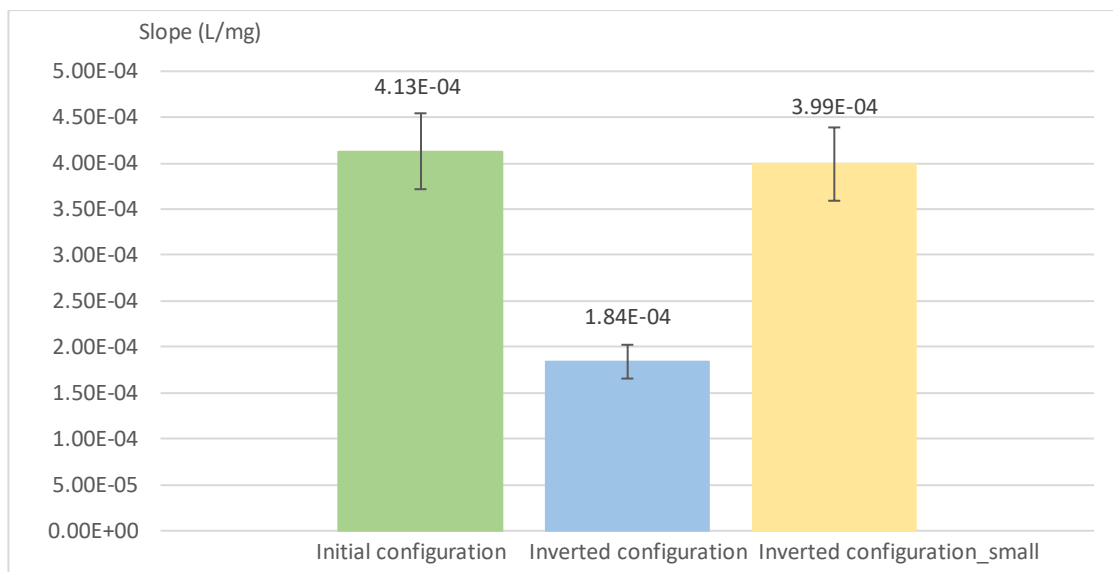


Figure 3.7 - Comparison of the sensitivity (calibration curve slope), for the different configurations of layers; Error bars represent a 10% deviation.

In the case of the inverted configuration\_small bar, the size of both discs was smaller (9.5 mm) and, subsequently, it couldn't absorb 20  $\mu\text{L}$ , and the sample volume inserted was 15  $\mu\text{L}$ . Despite having a smaller volume of sample, the sensitivity was not significantly different in comparison with the green bar. As so, the configuration chosen was the one presented in the yellow bar, with the same types of paper (Whatman 542 for the colour reagent layer and Whatman 1 for the reservoir), and discs of 9.5 mm. This happened because, in this assembly, the reagent was in the bottom layer and, consequently, more protected from degradation.

### 3.3. Colour Reaction Chemical Parameters Studies

#### 3.3.1. Hydroxide concentration

All the previous studies done in the  $\mu\text{PAD}$  were based on the concentrations of the solution described in the method developed by Sitanurak et al [50]. However, as this is an innovative device and it is different from the described study, the quantity of NaOH and picric acid were analysed, to improve the reaction between the creatinine (in standard/sample solution inserted) and the colour reagent in the layer. Hence, five NaOH concentrations were studied, maintaining a 0.030 M concentration of picric acid in the solution (Figure 3.8).

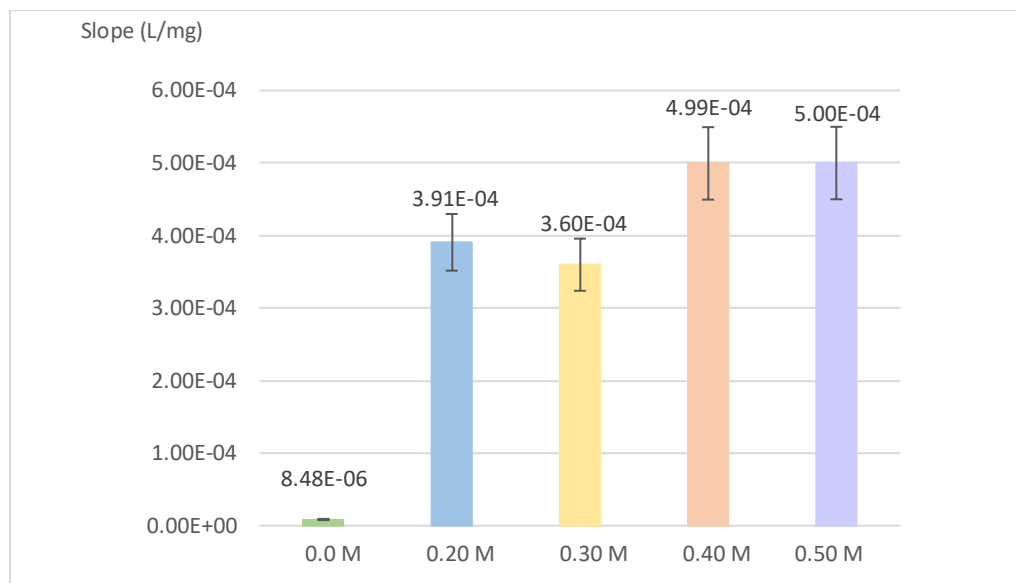


Figure 3.8 - Comparison of the sensitivity (calibration curve slope), for the different NaOH concentrations; Error bars represent a 10% deviation.

The results obtained show that the reaction doesn't occur without NaOH since it needs an alkaline medium. The concentrations that presented better sensitivity were 0.40 M and 0.50 M. As the difference between them is not significant, the concentration chosen was 0.40 M.

### 3.3.2. Picric acid concentration

Besides studying the influence on the calibration curve of the NaOH concentration, the concentration of picric acid was also analysed. The studied concentrations were 0.020 M, 0.030 M (as described by Sitanurak et al [50]), and 0.040 M (Figure 3.9).

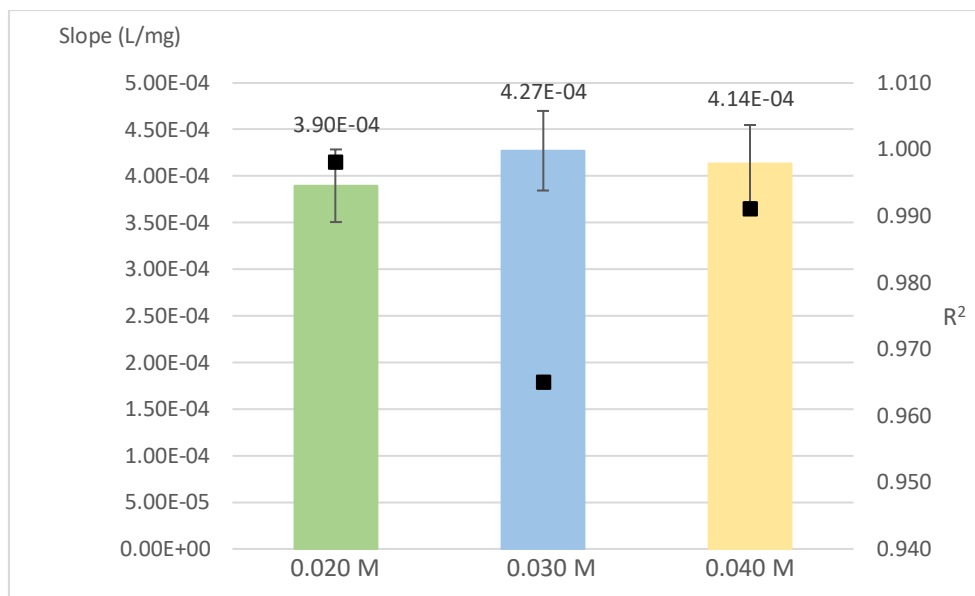


Figure 3.9 - Comparison of the sensitivity (calibration curve slope) and correlation coefficient (black dots), for the different Picric Acid concentrations; Error bars represent a 10% deviation.

When the slopes were compared, 0.030 M and 0.040 M of picric acid concentrations presented higher sensitivities. However, the calibration curve with 0.030 M of picric acid showed a correlation coefficient lesser than 0.990. So, this concentration was excluded, and the concentration 0.040 M was chosen.

Both reagents were mixed before the reaction to achieve an alkaline picrate solution. The mixture was prepared daily, due to its low-stability [49], while the picric acid was prepared weekly.

### 3.4. Standard/Sample Volume

The volume of sample was studied to see which one would result in a higher sensitivity of the device, and volumes of 15  $\mu\text{L}$ , 20  $\mu\text{L}$ , and 25  $\mu\text{L}$  were analysed. For the volumes of 20 and 25  $\mu\text{L}$ , the top layer thickness was increased (using Whatman 3 paper), because the  $\mu\text{PAD}$  couldn't absorb that amount of sample using Whatman 1.

Firstly, it was compared the volume of 15  $\mu\text{L}$  using Whatman 1 (W1\_15 $\mu\text{L}$ ) paper and Whatman 3 (W3\_15 $\mu\text{L}$ ) paper, with 20  $\mu\text{L}$  using Whatman 3 (W3\_20 $\mu\text{L}$ ), as shown in Figure 3.10.

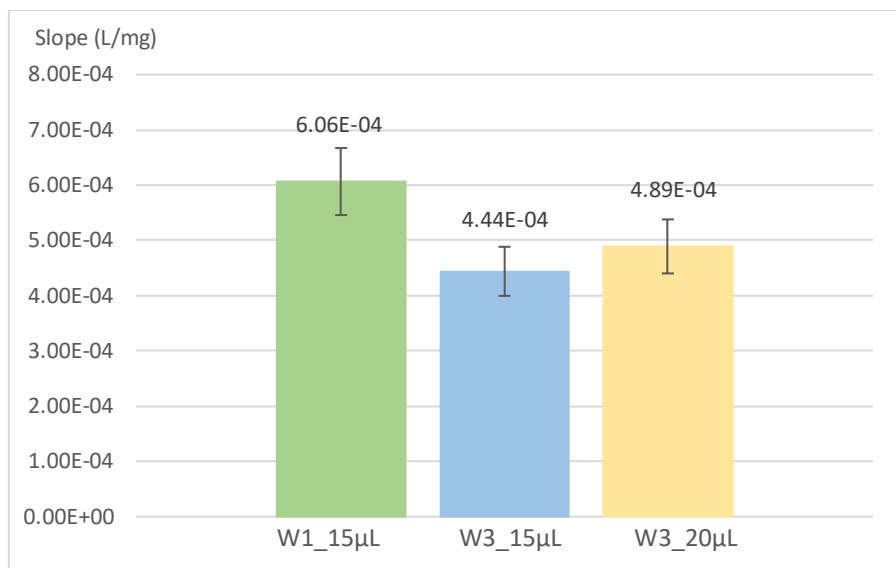


Figure 3.10 - Comparison of the sensitivity (calibration curve slope), for the different volumes of sample; Error bars represent a 10% deviation.

Since 15 µL of standard and using Whatman 1 was more sensitive, it was compared with even a higher volume of 25 µL, using Whatman 3 (W3\_25µL), to see if there was a significant change in the sensitivity (Figure 3.11).

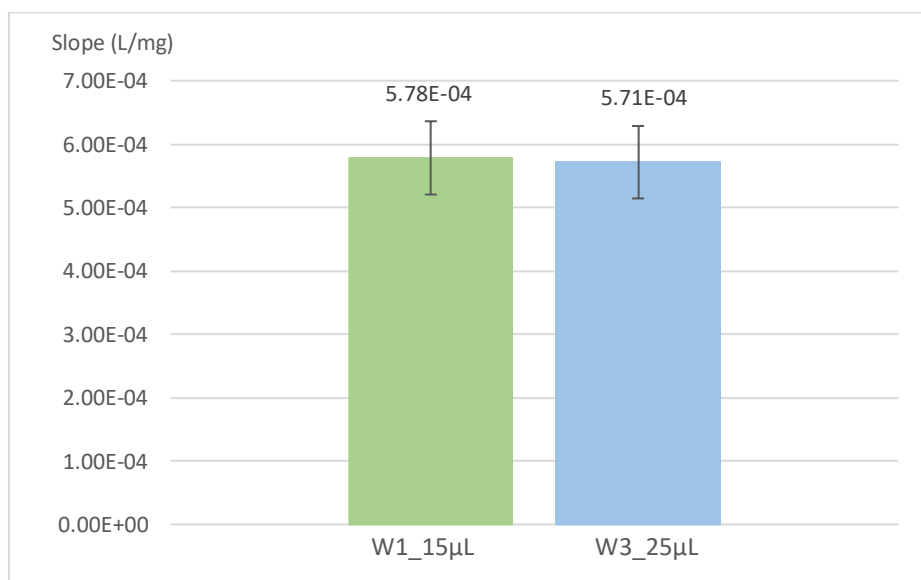


Figure 3.11 - Comparison of the sensitivity (calibration curve slope), for the different volumes of sample; Error bars represent a 10% deviation.

Analysing the results, both conditions didn't show a significant difference between sensitivities, and, because of that, the volume chosen was 15 µL (using Whatman 1 in the top layer), as it is a smaller volume and there was no necessity to spend more sample or standard.

It is important to mention that the standards were prepared daily and the respective stock solution every other day, due also to its low stability [49].

### 3.5. Stability Studies and Features

The developed device stability was assessed, as well as its other operational characteristics. It should be noted that, by analysing all the calibration curves, the concentration range was divided in two, one between 0 - 150 mg/L (0 to 15.0 mg/dL) and the other between 150 - 350 mg/L (15.0 to 35.0 mg/dL).

#### 3.5.1. $\mu$ PAD stability

Stability studies were performed testing different storage conditions before the sample insertion. As so, it was studied for how long it was possible to obtain linear calibration curves.

In terms of storage, the device was analysed when stored in an air, in a closed clear zip-locked bag in vacuum at room temperature and, later, also in vacuum but stored in the fridge (approximately 4°C). In all storage conditions, the  $\mu$ PAD was protected from the light by being wrapped around aluminium paper.

The periods of time studied were 2 days, 1 week (7 days) and 2 weeks (14 days) and, after that period of time, the standards were inserted as normally would be. Then, the results were compared with a freshly made  $\mu$ PAD to see if there were significant changes observed. The stability study is presented in Figure 3.12 and 3.13, for both limits of the calibration curve.

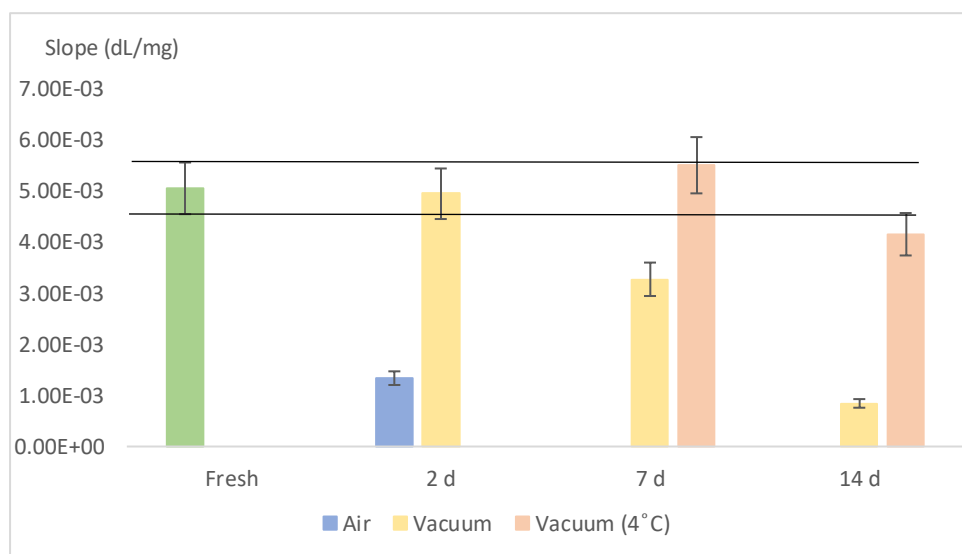


Figure 3.12 - Stability study of the  $\mu$ PAD for the lower range of concentrations (0 to 15.0 mg/dL); Error bars represent a 10% deviation, and the black horizontal lines represent the range of the error bars with a 10% deviation.

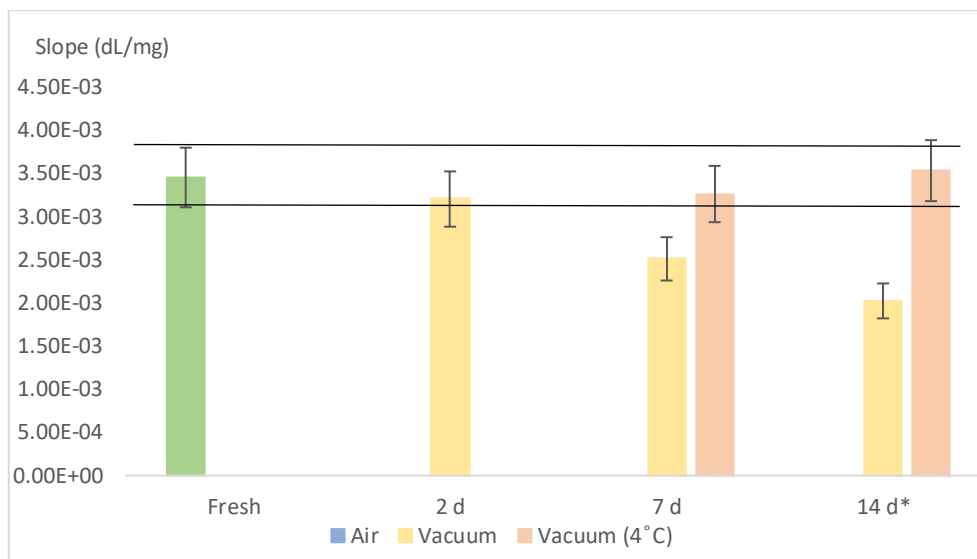


Figure 3.13 - Stability study of the  $\mu$ PAD for the higher range of concentrations (15.0 to 35.0 mg/dL); Error bars represent a 10% deviation, and the black horizontal lines represent the range of the error bars with a 10% deviation.

It was observed that, with storage in air, no calibration curve could be obtained with the device after 2 days. When looking at the storage of vacuum at room temperature, it is possible to see that after 2 days, the calibration curve slope remained within a  $\pm 10\%$  deviation and there are no significant differences. However, after 1 week, this storage was no longer suitable since it is possible to observe significant differences between the sensitivities of these  $\mu$ PADs and the freshly made  $\mu$ PAD.

In the case of storing in vacuum refrigerated (at 4°C), this was introduced at one week due to the observed loss of sensitivity of the storage in vacuum at room temperature. This proved to be not significantly different when compared with the freshly made one ( $< 10\%$  deviation). However, at two weeks, for the lower range of concentrations, there are significant differences when comparing to the fresh  $\mu$ PAD and, although the differences in the higher range of concentrations (\*) are not significant, the calibration curve, in this case, was made with a fewer number of standards and, therefore, the  $\mu$ PAD would not be able to quantify creatinine as it should. Hence, the  $\mu$ PAD can be fabricated and stored for up to one week, if it is in a closed clear zip-locked bag, in vacuum, and stored in the fridge.

### 3.5.2. Stability of the reaction product

After inserting the standard or sample in the device, a reaction product is obtained. As so, in order to study the stability of this coloured product, a typical calibration curve was prepared and scanned within different periods of time: 20 minutes (20'), 40 minutes (40'), 1 hour (60'), 1h30 hours (90'), 2 hours (120'), 2h30 hours (150'), 3 hours (180'), 4 hours (240')

and 6 hours (360'). The sensitivities achieved in these different scans were compared with each other, as it is present in Figure 3.14.

By observing Figure 3.14, it is possible to conclude that the sensitivity increases until 40 minutes and it is stable for 4 hours (180'). The slope of the reaction time of 6 hours (360') is not included in the 10% range, which means that the product isn't stable in that period of time and, therefore, it loses its stability after 4 hours.

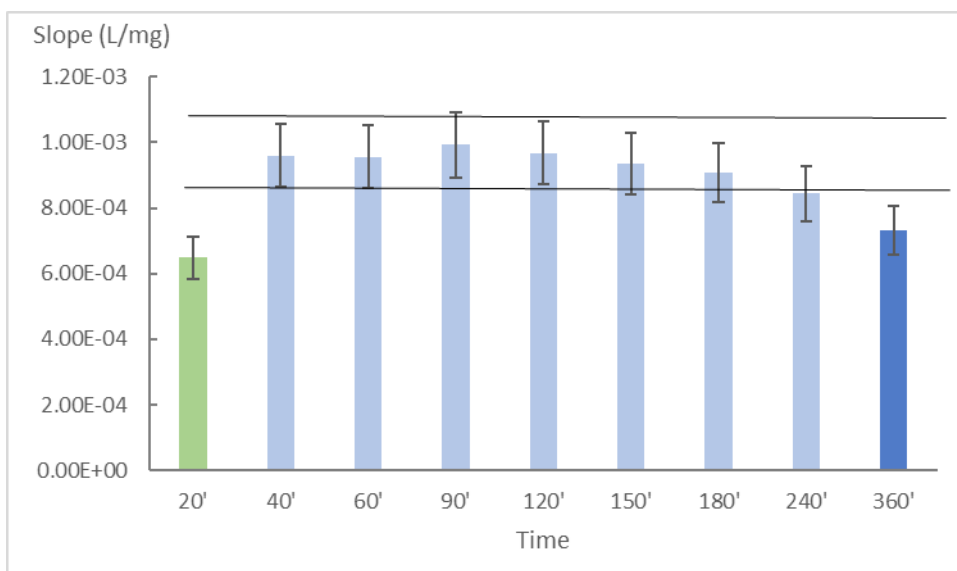


Figure 3.14 – Reaction product stability. Error bars represent a 10% deviation, and the black horizontal lines represent the range of the error bars with a 10% deviation.

It is also possible to notice that the reaction time represented in green (20'), which is the chosen reading time of the  $\mu$ PAD, shows less sensitivity than 40 minutes. Nevertheless, when reading the standards or samples in the device after 20 minutes, the calibration curves obtained were still sensitive enough to read samples with accuracy, as will be demonstrated in section 3.6.

### 3.5.3. Features of the $\mu$ PAD

After optimizing all the parameters studied in the  $\mu$ PAD, a table of its features is presented in Table 3.1, containing: the dynamic ranges of creatinine quantification; the typical calibration curves for the separate intervals of the dynamic range; the limit of detection (LOD); the limit of quantification (LOQ); the relative standard deviation (RSD) for the  $\mu$ PAD (interday) and for the sample analysis; the ideal time to scan; and the consumption of reagents and sample per both calibration curves.



Table 3.1 - Features of the developed  $\mu$ PAD for creatinine determination in urine samples.

Dynamic range	2.20 - 15.0 mg/dL (22.0 - 150 mg/L)
	15.0 - 35.0 mg/dL (150 - 350 mg/L)
Typical calibration curves <sup>a</sup> (A = slope x [Creatinine] + b)	<ul style="list-style-type: none"> <li>For the lower range: A = 0.00550 ± 0.00020 x [Creatinine] + 0.001 ± 0.001</li> <li>For the higher range: A = 0.00340 ± 0.00030 x [Creatinine] + 0.030 ± 0.008</li> </ul>
LOD (mg/dL)	0.66
LOQ (mg/dL)	2.20
RSD (%) - $\mu$ PAD <sup>a</sup> Repeatability	<ul style="list-style-type: none"> <li>4% (For the lower range)</li> <li>9% (For the higher range)</li> </ul>
RSD (%) – Sample <sup>b</sup> Precision	<ul style="list-style-type: none"> <li>10.5 % (3.40 ± 0.38 mg/dL)</li> <li>11.8% (15.40 ± 0.43 mg/dL)</li> </ul>
Time to scan	20 minutes (up to 4 hours)
Reagent consumption / $\mu$ PAD (mg)	<ul style="list-style-type: none"> <li>Picric acid: 3.59</li> <li>Sodium hydroxide: 4.80</li> </ul>
Sample consumption <sup>c</sup> ( $\mu$ L)	90

<sup>a</sup> n=8 calibration curves

<sup>b</sup> #10 readings per sample

<sup>c</sup> per analysis (#6 readings)

It is important to mention that the dynamic range was studied with the purpose of making it larger (until 50.0 mg/dL). However, the superior limit was set at 35.0 mg/dL, due to issues with linearity (Appendix A). Also, there are two typical calibration curves for 2 intervals of the creatinine concentrations (2.20 - 15.0 mg/dL and 15.0 - 35.0 mg/dL), since it was noted that there were two different sensitivities. The equations present in Table 3.1 were the result of 8 calibration curves, made in different days, but under the same design conditions.

According to IUPAC recommendations [51], the limit of detection (LOD) was calculated as:

$$LOD = 3 \times \frac{\text{Standard deviation of the calibration curve intercept}}{\text{Slope of the calibration curve}}$$

and the limit of quantification (LOQ) as:

$$LOQ = 10 \times \frac{\text{Standard deviation of the calibration curve intercept}}{\text{Slope of the calibration curve}}$$

The repeatability of the device was analysed through the RSD of the  $\mu$ PAD, also considering 8 calibration curves made in different days (the calibration curves are present in Appendix B). The precision analysis of the  $\mu$ PAD was studied through the RSD of the two distinct  $\mu$ PADs, after inserting 2 samples, both a slightly higher to the inferior limit of each dynamic range (close to 2.20 mg/dL and close to 15.0 mg/dL) and using 10 measurements of that samples.

The consumption of reagents was calculated from the volume of reagent solution used per  $\mu$ PAD therefore, per two  $\mu$ PADs (one complete calibration curve), it would be the double. The presented sample consumption corresponds to one determination, which requires #6 readings.

### 3.6. Application to Samples

#### 3.6.1. Matrix interference assessment

After the previous studies and before applying the  $\mu$ PAD to biological samples, an interference of the matrix assessment was performed, to see if the urine matrix would significantly affect the device when compared with Milli-Q water. Therefore, two calibration curves were made, one using standards prepared with Milli-Q water (H<sub>2</sub>O).and the other with synthetic urine [52]. The results are shown in Figure 3.15.

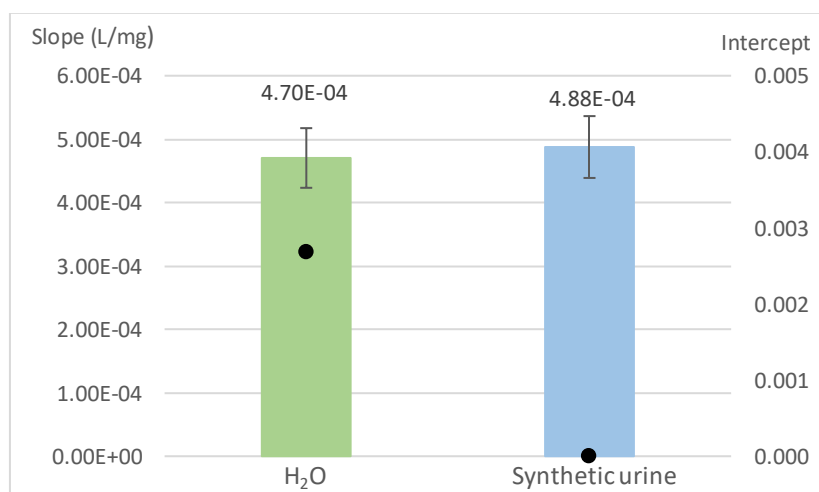


Figure 3.15 - Comparison of the sensitivity (calibration curve slope) between H<sub>2</sub>O and Synthetic Urine, as well as the absorbance blank values for each matrix (black dots); Error bars represent a 10% deviation.

Analysing the previous figure, it was possible to conclude that the slopes weren't significantly different from each other, as well as the intercept values, which are both approximately equal to 0. It is possible to conclude that the components of the urine matrix do not interfere with the reaction. Therefore, the Milli-Q water was chosen for the matrix, as it is easier to dilute the urine samples for the sample application in the device.

### 3.6.2. Accuracy assessment

After having established the features of the developed device, its accuracy assessment was performed. The results validation was attained analysing several (#16) urine samples with the  $\mu$ PAD and the comparative procedure (batchwise method). The concentration of creatinine in each sample was determined and the relative deviation between both methods ( $[\text{Creatinine}]_{\text{CM}}$  and  $[\text{Creatinine}]_{\mu\text{PAD}}$ ) was calculated. The results obtained are presented in Table 3.2.

Table 3.2 – Comparison of the results obtained with the developed  $\mu$ PAD and a comparative method (CM) by calculating the relative deviation percentage (%RD); SD, standard deviation.

<i>Assay</i>	<i>[Creatinine]<sub>CM</sub> ± SD (mg/dL)</i>	<i>[Creatinine]<sub>μPAD</sub> ± SD (mg/dL)</i>	<i>%RD</i>
<b>1</b>	22.3 ± 0.1	21.2 ± 1.6	-5.0
<b>2</b>	23.6 ± 0.2	22.9 ± 1.6	-3.0
<b>3</b>	13.4 ± 0.2	15.3 ± 0.7	15
<b>4</b>	16.1 ± 0.2	13.3 ± 0.9	-18
<b>5</b>	6.30 ± 0.04	6.80 ± 0.38	7.9
<b>6</b>	14.5 ± 0.1	11.7 ± 0.9	-20
<b>7</b>	21.6 ± 0.1	20.5 ± 1.2	-5.2
<b>8</b>	9.78 ± 0.12	10.3 ± 0.2	5.3
<b>9</b>	9.11 ± 0.08	9.80 ± 0.58	7.6
<b>10</b>	13.0 ± 0.2	12.4 ± 1.1	-4.6
<b>11</b>	11.7 ± 0.3	12.2 ± 0.7	4.1
<b>12</b>	13.3 ± 0.1	14.2 ± 0.5	7.1
<b>13</b>	15.5 ± 0.1	15.4 ± 0.4	-0.5
<b>14</b>	11.4 ± 0.1	11.2 ± 0.9	-2.0
<b>15</b>	8.57 ± 0.26	9.20 ± 0.99	7.4
<b>16</b>	12.2 ± 0.3	12.2 ± 1.8	0.2

All the analysed samples presented creatinine concentrations within the limits of the developed  $\mu$ PAD. A linear relationship between the two methods was established (Appendix C) and the obtained equation (where the values in brackets represent the 95% confidence interval),

$$[\text{Creatinine}]_{\mu\text{PAD}} = 0.873 (\pm 0.129) [\text{Creatinine}]_{\text{CM}} + 1.52 (\pm 1.89)$$

proved that the developed method is not significantly different from the comparative method since both the slope and intercept were not statistically different from 1 and 0 respectively.

## 4. COST ANALYSIS

With the purpose of developing a fast sensitive device but also low-cost for the determination of creatinine, the prices of the consumables used in its assembly were accounted for.

Each  $\mu$ PAD used 24 disc-units and, subsequently, 24 discs of Whatman 542 paper and 24 discs of Whatman 1 paper. Also, it used 1 plastic pouch and 288  $\mu$ L of colour reagent solution (12  $\mu$ L per disc in the reagent layer). All the calculations of these prices are presented in Appendix D and the respective cost per  $\mu$ PAD is present in Table 4.1.

*Table 4.1 - Price of the consumables used in the  $\mu$ PAD and the total price per unit.*

<i>Filter Paper</i>		<i>Plastic Pouch</i>	<i>Reagent</i>	<i>Total</i>
<b>Whatman 542</b>	<b>Whatman 1</b>			
0.330 €	0.022 €	0.046 €	0.0029 €	≈ 0.40 €

## 5. CONCLUSION

A novel microfluidic paper-based analytical device ( $\mu$ PAD) was developed with success. The primary aim of this work was to create a device that provides a simple, fast, on-site, easy-to-use, and inexpensive diagnosis of health conditions associated with creatinine levels in urine samples. The  $\mu$ PAD follows the ASSURED guidelines of the World Health Organization and, for that reason, can be applied in developing countries and areas, for the population that doesn't have access to basic health care and resources. Besides that, the developed  $\mu$ PAD is environmentally friendly, producing a low quantity of waste and being easy to dispose by incineration, important advantages when compared with other analysis procedures.

After studying all the parameters and optimizing the method, the final configuration of the  $\mu$ PAD consisted in two layers of filter paper discs of 9,5 mm of diameter. The top layer (Whatman 1) was used as a reservoir and the bottom layer (Whatman 542) contained the colour reagent solution (12  $\mu$ L of alkaline picric acid). The filter papers were aligned into a laminating plastic pouch and 15  $\mu$ L of standard/sample were inserted through a 3 mm hole in the plastic pouch. This represents another advantage of this device since the amounts of sample and reagent used are reduced. To determine creatinine, after the sample placement, a simple scanning of the  $\mu$ PAD after 20 minutes and posterior image processing in ImageJ (free software), allowed to measure the intensity of the colour developed, and calculate the absorbance using the blank signal as a pseudo incident radiation ( $I_0$ ).

To verify if this device would be suitable for transportation, a stability study was performed, concluding that the  $\mu$ PAD enabled the accurate creatinine determination for one week, when stored in vacuum and at approximately 4°C. The stability of the reaction product was also assessed, and it was proved that the reading could be made up to 4 hours after placing the sample. Also, it is noticeable that the device is more sensitive at 40 minutes than at 20 minutes. However, one of the main goals of developing this  $\mu$ PAD is to achieve a rapid diagnosis and, for that reason, the scanning at 20 minutes was chosen. Moreover, even though it presented a smaller value of sensitivity, the value is already suitable to read biological samples and achieve good calibration curves, as it was observed further on.

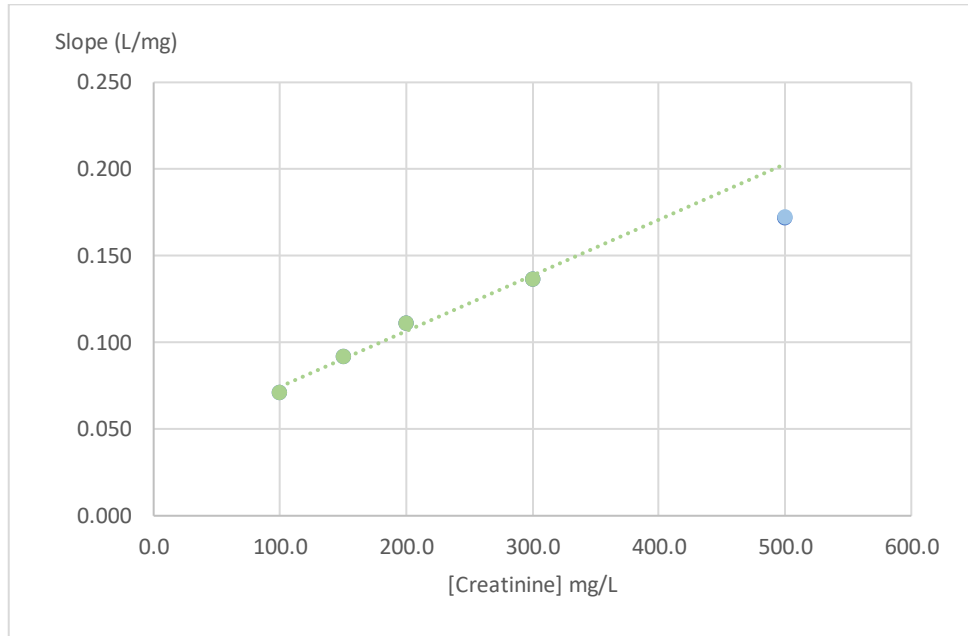
This paper approach allowed quantification of creatinine within the dynamic range of 2.20 mg/dL to 35.0 mg/dL, divided into two distinct ranges with different calibration curves, one for 2.20 - 15.0 mg/dL ( $A = 0.00550 (\pm 0.0002) \times [\text{Creatinine}] \text{ mg/dL} + 0.00100 (\pm 0.001)$ ) and the other for 15.0 - 35.0 mg/dL ( $A = 0.00340 (\pm 0.0003) \times [\text{Creatinine}] \text{ mg/dL} + 0.0300 (\pm 0.008)$ ). The  $\mu$ PAD method enabled a limit of detection (LOD) and quantification (LOQ) of 0.66 mg/dL and 2.20 mg/dL, respectively, which is in line with the values expected in urine sample.

With the purpose of validating the developed method, urine samples were analysed with the  $\mu$ PAD and with a comparative method (batchwise) and it was concluded that there were no significant differences between both methods. Nonetheless, before performing this validation, a matrix interference study was done, where standards made with Milli-Q water were compared with standards made with synthetic urine. It was possible to conclude that there were no statistically significant differences between both matrices and the matrix chosen was Milli-Q water since it is easier to manage.

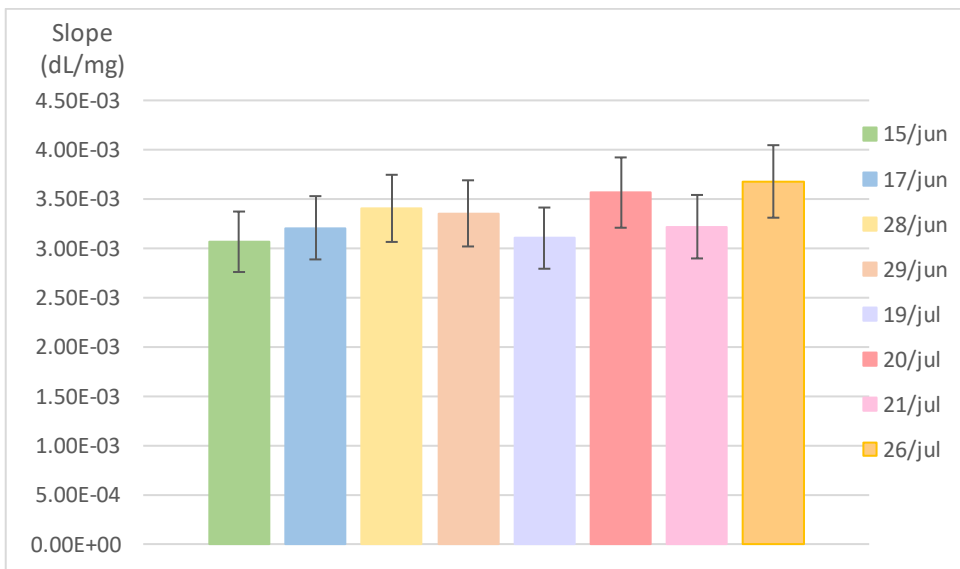
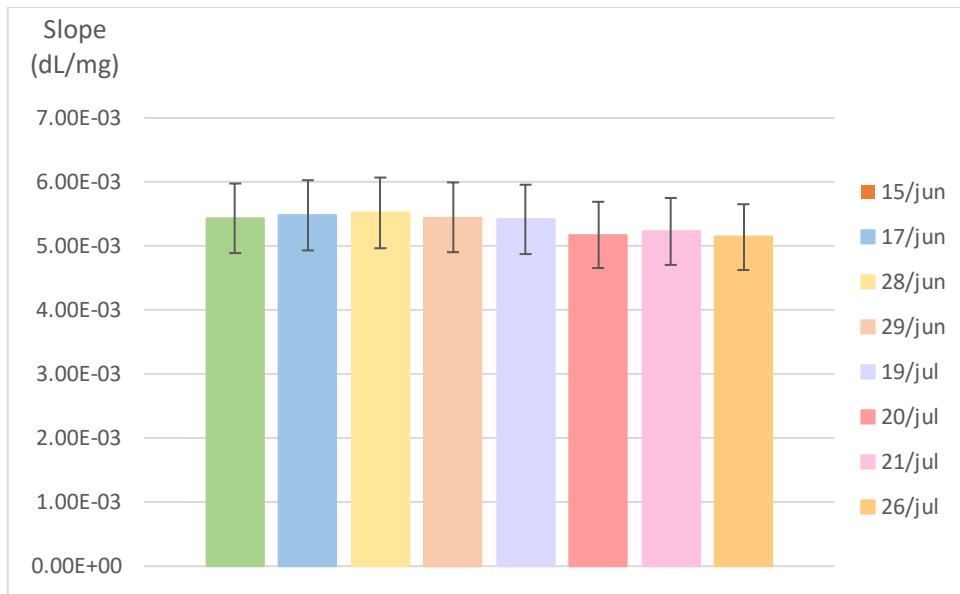
To conclude, all the features of this  $\mu$ PAD indicate that this is, in fact, an innovative and effective device for the diagnosis of health conditions linked with creatinine, as it is the case of kidney-associated diseases. Combined with the fact that the developed method proved to be simple, user-friendly, disposable, and portable, it is a low-cost method when compared with conventional biological procedures, as it costs less than 0.50 € (accounting just the consumables) and is suitable for point of care and on-location analysis.

## 6. APPENDIX

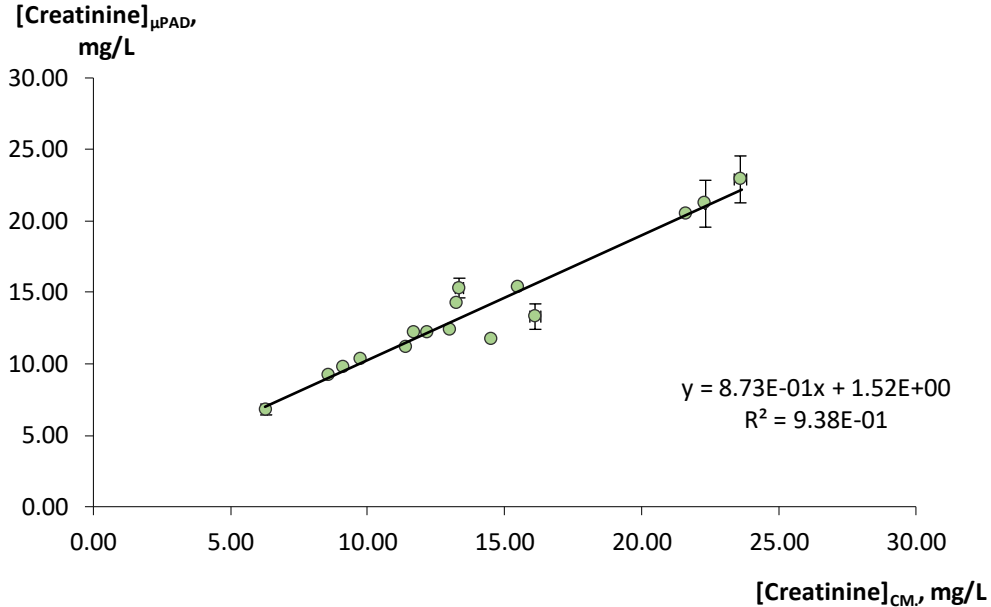
**Appendix A** – Assessment of the maximum creatinine limit within the  $\mu$ PAD calibration curve.



**Appendix B** – Interday calibration curve slopes, used to calculate the  $\mu$ PAD features; A) range 0 - 15.0 mg/dL of Creatinine; B) range 15.0 - 35.0 mg/dL of Creatinine; Error bars represent 10% deviation



**Appendix C** – Linear relationship between the creatine values in the analysed urine samples with the developed  $\mu$ PAD ( $[\text{Creatinine}]_{\mu\text{PAD}}$ ) and the comparative method ( $[\text{Creatinine}]_{\text{CM}}$ ).



**Appendix D – Cost analysis calculations.**

Type of paper	Disc diameter (cm)	Paper diameter (cm)	Box price (€)	Nr. of sheets per box	Price per sheet (€)	Nr. of discs per sheet	Price per disc (€)	Price per layer (€) (price per disc x 24)
<b>W1</b>	0.95	15	14.72	100	0.1472	164	0.0009	<b>0.022</b>
<b>W542</b>	0.95	9	66.03	100	0.6603	48	0.0138	<b>0.330</b>

Plastic pouches box price (€)	Nr of pouches per box	Price per pouch (€)
4.55	100	<b>0.046</b>

Reagent	Price per flask (€)	Quantity per flask (g)	Price / gram (€)
<b>Picric Acid</b>	60.4	100	0.604
<b>NaOH</b>	27.5	100	0.274

Reagent	Reagent concentration (M)	Reagent concentration (g/L)	Quantity / $\mu$ PAD* (g)	Price / grams of reagent / $\mu$ PAD (€)	Total price of reagents / $\mu$ PAD (€)
<b>Picric Acid</b>	0.0400	9.16	0.0026 g	0.00159	0.0029
<b>NaOH</b>	0.400	16.0	0.0046 g	0.00127	

\*12  $\mu$ L / disc x 24 discs

## 7. BIBLIOGRAPHY

- [1] C. S. Pundir, P. Kumar, and R. Jaiwal, “Biosensing methods for determination of creatinine: A review,” *Biosensors and Bioelectronics*, vol. 126. Elsevier, pp. 707–724, Feb. 01, 2019, doi: 10.1016/j.bios.2018.11.031.
- [2] S. Narayanan and H. D. Appleton, “Creatinine: A review,” *Clinical Chemistry*, vol. 26, no. 8. Oxford Academic, pp. 1119–1126, Jul. 01, 1980, doi: 10.1093/clinchem/26.8.1119.
- [3] J. H. Salazar, “Overview of urea and creatinine,” *Lab Medicine*, vol. 45, no. 1. Oxford Academic, pp. e19–e20, Feb. 01, 2014, doi: 10.1309/LM920SBNZPJRGUT.
- [4] J. F. Moore and J. D. Sharer, “Methods for quantitative creatinine determination,” *Curr. Protoc. Hum. Genet.*, vol. 2017, no. 1, p. A.30.1-A.30.7, Apr. 2017, doi: 10.1002/cphg.38.
- [5] C. Hersey-Benner and J. Mayer, “Creatinine,” in *Clinical Veterinary Advisor: Birds and Exotic Pets*, W.B. Saunders, 2012, pp. 615–615.
- [6] E. P. Randviir and C. E. Banks, “Analytical methods for quantifying creatinine within biological media,” *Sensors and Actuators, B: Chemical*, vol. 183. Elsevier, pp. 239–252, Jul. 05, 2013, doi: 10.1016/j.snb.2013.03.103.
- [7] C. P. Davis, “Creatinine Blood Test: Normal, Low, High Levels, Causes & Symptoms,” 2022. [https://www.medicinenet.com/creatinine\\_blood\\_test/article.htm](https://www.medicinenet.com/creatinine_blood_test/article.htm) (accessed Jun. 09, 2022).
- [8] M. D. MILNE, “TUBULAR REABSORPTION AND SECRETION.,” *J. Clin. Pathol.*, vol. 18, pp. 515–519, Jan. 1965, doi: 10.1016/b978-0-12-800883-6.00072-0.
- [9] Y. Xue, L. B. Daniels, A. S. Maisel, and N. Iqbal, “Cardiac Biomarkers,” in *Reference Module in Biomedical Sciences*, Elsevier, 2014.
- [10] M. Eng, “Urine Creatinine Test Normal Range + Low & High Levels,” 2021. <https://labs.selfdecode.com/blog/creatinine-urine-test/> (accessed Jun. 07, 2022).
- [11] “The Royal College of Physicians and Surgeons of Canada Le College Royal Des Medecins Et Chirurgiens Du Canada,” *Can. J. Psychiatry*, vol. 25, no. 6, pp. 532–533, 1980, doi: 10.1177/070674378002500625.
- [12] A. L. Brantsæter *et al.*, “Inadequate iodine intake in population groups defined by age, life stage and vegetarian dietary practice in a norwegian convenience sample,” *Nutrients*, vol. 10, no. 2, 2018, doi: 10.3390/nu10020230.
- [13] R. Amin, S.-Y. Ahn, and A. Moudgil, “Kidney and urinary tract disorders,” in *Biochemical and Molecular Basis of Pediatric Disease*, Academic Press, 2021, pp. 167–228.
- [14] C. J. Diskin, “Creatinine and glomerular filtration rate: Evolution of an accommodation,” *Annals of Clinical Biochemistry*, vol. 44, no. 1. pp. 16–19, 2007, doi: 10.1258/000456307779595940.

- [15] G. Ciarimboli *et al.*, “Proximal tubular secretion of creatinine by organic cation transporter OCT2 in cancer patients,” *Clin. Cancer Res.*, vol. 18, no. 4, pp. 1101–1108, Feb. 2012, doi: 10.1158/1078-0432.CCR-11-2503.
- [16] “Creatinine (English) - Medical terminology for medical students,” 2020. <https://www.youtube.com/watch?v=h5plvEYjNP8> (accessed Jun. 13, 2022).
- [17] D. B. Barr, L. C. Wilder, S. P. Caudill, A. J. Gonzalez, L. L. Needham, and J. L. Pirkle, “Urinary creatinine concentrations in the U.S. population: Implications for urinary biologic monitoring measurements,” *Environ. Health Perspect.*, vol. 113, no. 2, pp. 192–200, Feb. 2005, doi: 10.1289/ehp.7337.
- [18] E. Tynkevich *et al.*, “Decrease in urinary creatinine excretion in early stage chronic kidney disease,” *PLoS One*, vol. 9, no. 11, Nov. 2014, doi: 10.1371/journal.pone.0111949.
- [19] H. A. Polinder-Bos, H. Nacak, F. W. Dekker, S. J. L. Bakker, C. A. J. M. Gaillard, and R. T. Gansevoort, “Low Urinary Creatinine Excretion Is Associated With Self-Reported Frailty in Patients With Advanced Chronic Kidney Disease,” *J. Comput. Des. Eng.*, vol. 4, no. 3, pp. 676–685, Jul. 2017, doi: 10.1016/j.ekir.2017.02.021.
- [20] A. Ortiz, M. D. Sanchez-Niño, and A. B. Sanz, “The meaning of urinary creatinine concentration,” *Kidney International*, vol. 79, no. 7. Elsevier, p. 791, Apr. 01, 2011, doi: 10.1038/ki.2011.1.
- [21] N. M. Paige and G. T. Nagami, “The top 10 things nephrologists wish every primary care physician knew,” *Mayo Clinic Proceedings*, vol. 84, no. 2. Mayo Foundation, pp. 180–186, 2009, doi: 10.4065/84.2.180.
- [22] K. Kalantari and W. Kline Bolton, “A good reason to measure 24-hour urine creatinine excretion, but not to assess kidney function,” *Clinical Journal of the American Society of Nephrology*, vol. 8, no. 11. American Society of Nephrology, pp. 1847–1849, Nov. 11, 2013, doi: 10.2215/CJN.09770913.
- [23] I. Helal, G. M. Fick-Brosnahan, B. Reed-Gitomer, and R. W. Schrier, “Glomerular hyperfiltration: Definitions, mechanisms and clinical implications,” *Nature Reviews Nephrology*, vol. 8, no. 5. Nat Rev Nephrol, pp. 293–300, May 2012, doi: 10.1038/nrneph.2012.19.
- [24] MedlinePlus, “Creatinine Test: MedlinePlus Medical Test,” *medlineplus.gov*, 2020. <https://medlineplus.gov/lab-tests/creatinine-test/> (accessed Jun. 15, 2022).
- [25] “Creatinine Urine Test: Understanding the Test and Results,” 2017. <https://www.healthline.com/health/creatinine-clearance> (accessed Jun. 12, 2022).
- [26] “Urine Collection Protocol,” p. 3062, 2016.
- [27] R. Narimani, M. Esmaeili, S. H. Rasta, H. T. Khosroshahi, and A. Mobed, “Trend in creatinine determining methods: Conventional methods to molecular-based methods,” *Anal. Sci. Adv.*, vol. 2, no. 5–6, pp. 308–325, Jun. 2021, doi: 10.1002/ansa.202000074.
- [28] H. Husdan and A. Rapoport, “Estimation of creatinine by the Jaffe reaction. A comparison of three methods.,” *Clin. Chem.*, vol. 14, no. 3, pp. 222–238, 1968, doi: 10.1093/clinchem/14.3.222.

- [29] G. M. Fernandes *et al.*, “Novel approaches for colorimetric measurements in analytical chemistry – A review,” *Analytica Chimica Acta*, vol. 1135. Elsevier, pp. 187–203, Oct. 23, 2020, doi: 10.1016/j.aca.2020.07.030.
- [30] E. L. Rossini, M. I. Milani, E. Carrilho, L. Pezza, and H. R. Pezza, “Simultaneous determination of renal function biomarkers in urine using a validated paper-based microfluidic analytical device,” *Anal. Chim. Acta*, vol. 997, pp. 16–23, 2018, doi: 10.1016/j.aca.2017.10.018.
- [31] T. Küme, B. Sağlam, C. Ergon, and A. R. Sisman, “Evaluation and comparison of Abbott Jaffe and enzymatic creatinine methods: Could the old method meet the new requirements?,” *J. Clin. Lab. Anal.*, vol. 32, no. 1, Jan. 2018, doi: 10.1002/jcla.22168.
- [32] J. G. H. Cook, “Factors Influencing the Assay of Creatinine,” vol. 12, no. 36, pp. 219–232, 1975.
- [33] J. R. Delanghe and M. M. Speeckaert, “Creatinine determination according to Jaffe - What does it stand for?,” *NDT Plus*, vol. 4, no. 2, pp. 83–86, Apr. 2011, doi: 10.1093/ndtplus/sfq211.
- [34] C. Hu, F. E. Muller-Karger, and R. G. Zepp, “Absorbance, absorption coefficient, and apparent quantum yield: A comment on common ambiguity in the use of these optical concepts,” *Limnol. Oceanogr.*, vol. 47, no. 4, pp. 1261–1267, Jul. 2002, doi: 10.4319/lo.2002.47.4.1261.
- [35] P. Lisowski and P. K. Zarzycki, “Microfluidic paper-based analytical devices ( $\mu$ PADs) and micro total analysis systems ( $\mu$ TAS): Development, applications and future trends,” *Chromatographia*, vol. 76, no. 19–20. Springer, pp. 1201–1214, Oct. 2013, doi: 10.1007/s10337-013-2413-y.
- [36] C. S. Kosack, A. L. Page, and P. R. Klatser, “A guide to aid the selection of diagnostic tests,” *Bull. World Health Organ.*, vol. 95, no. 9, pp. 639–645, Sep. 2017, doi: 10.2471/BLT.16.187468.
- [37] Y. Yang, E. Noviana, M. P. Nguyen, B. J. Geiss, D. S. Dandy, and C. S. Henry, “Paper-Based Microfluidic Devices: Emerging Themes and Applications,” *Analytical Chemistry*, vol. 89, no. 1. American Chemical Society, pp. 71–91, Jan. 03, 2017, doi: 10.1021/acs.analchem.6b04581.
- [38] L. M. Fu and Y. N. Wang, “Detection methods and applications of microfluidic paper-based analytical devices,” *TrAC - Trends in Analytical Chemistry*, vol. 107. Elsevier, pp. 196–211, Oct. 01, 2018, doi: 10.1016/j.trac.2018.08.018.
- [39] A. W. Martinez, S. T. Phillips, M. J. Butte, and G. M. Whitesides, “Patterned paper as a platform for inexpensive, low-volume, portable bioassays,” *Angew. Chemie - Int. Ed.*, vol. 46, no. 8, pp. 1318–1320, 2007, doi: 10.1002/anie.200603817.
- [40] M. I. G. S. Almeida, B. M. Jayawardane, S. D. Kolev, and I. D. McKelvie, “Developments of microfluidic paper-based analytical devices ( $\mu$ PADs) for water analysis: A review,” *Talanta*, vol. 177, pp. 176–190, Jan. 2018, doi: 10.1016/j.talanta.2017.08.072.

- [41] F. T. S. M. Ferreira, R. B. R. Mesquita, and A. O. S. S. Rangel, "Novel microfluidic paper-based analytical devices ( $\mu$ PADs) for the determination of nitrate and nitrite in human saliva," *Talanta*, vol. 219, no. April, p. 121183, 2020, doi: 10.1016/j.talanta.2020.121183.
- [42] J. I. S. Aguiar *et al.*, "Development of a microfluidic paper-based analytical device for magnesium determination in saliva samples," *Talanta Open*, vol. 6, no. August, 2022, doi: 10.1016/j.talo.2022.100135.
- [43] E. Noviana *et al.*, "Microfluidic Paper-Based Analytical Devices: From Design to Applications," *Chemical Reviews*, vol. 121, no. 19. American Chemical Society, pp. 11835–11885, Oct. 13, 2021, doi: 10.1021/acs.chemrev.0c01335.
- [44] S. Nishat, A. T. Jafry, A. W. Martinez, and F. R. Awan, "Paper-based microfluidics: Simplified fabrication and assay methods," *Sensors Actuators, B Chem.*, vol. 336, p. 129681, Jun. 2021, doi: 10.1016/j.snb.2021.129681.
- [45] X. Li, J. Tian, and W. Shen, "Quantitative biomarker assay with microfluidic paper-based analytical devices," *Anal. Bioanal. Chem.*, vol. 396, no. 1, pp. 495–501, 2010, doi: 10.1007/s00216-009-3195-9.
- [46] N. C. Birch and D. F. Stickle, "Example of use of a desktop scanner for data acquisition in a colorimetric assay [2]," *Clinica Chimica Acta*, vol. 333, no. 1–2. Clin Chim Acta, pp. 95–96, Jul. 01, 2003, doi: 10.1016/S0009-8981(03)00168-2.
- [47] B. M. Jayawardane, S. Wei, I. D. McKelvie, and S. D. Kolev, "Microfluidic paper-based analytical device for the determination of nitrite and nitrate," *Anal. Chem.*, vol. 86, no. 15, pp. 7274–7279, 2014, doi: 10.1021/ac5013249.
- [48] Y. Thepchuay, R. B. R. Mesquita, D. Nacapricha, and A. O. S. S. Rangel, "Micro-PAD card for measuring total ammonia nitrogen in saliva," *Anal. Bioanal. Chem.*, vol. 412, no. 13, pp. 3167–3176, 2020, doi: 10.1007/s00216-020-02577-w.
- [49] A. Machado, A. A. Bordalo, and R. B. R. Mesquita, "Sequential injection method for the biparametric determination of Iodine and Creatinine in urine." Krakow, Poland, 2021.
- [50] J. Sitanurak, P. Inpota, T. Mantim, N. Ratanawimarnwong, P. Wilairat, and D. Nacapricha, "Simultaneous determination of iodide and creatinine in human urine by flow analysis with an on-line sample treatment column," *Analyst*, vol. 140, no. 1, pp. 295–302, 2015, doi: 10.1039/c4an01224k.
- [51] L. A. Currie, "Nomenclature in evaluation of analytical methods including detection and quantification capabilities," *Pure Appl. Chem.*, vol. 67, no. 10, pp. 1699–1723, Jan. 1995, doi: 10.1351/pac199567101699.
- [52] T. Brooks and C. W. Keevil, "A simple artificial urine for the growth of urinary pathogens," *Lett. Appl. Microbiol.*, vol. 24, no. 3, pp. 203–206, 1997, doi: 10.1046/j.1472-765X.1997.00378.x.